Journal of Quantitative Spectroscopy & Radiative Transfer 338 (2025) 109427

Contents lists available at ScienceDirect

Journal of Quantitative Spectroscopy and Radiative Transfer

journal homepage: www.elsevier.com/locate/jqsrt

Advances in polarization imaging: Techniques and instrumentation

Vipin Tiwari

Institute of Physics, University of Tartu, W. Ostwaldi 1, 50411 Tartu, Estonia

ARTICLE INFO

Keywords:
Polarization imaging
Stokes polarimetry
Jones matrix
Mueller matrix
Polarization camera
Spatial light modulator

ABSTRACT

Polarization imaging has drawn significant attention from the research fraternity for decades due to its prominent imaging capabilities across multidisciplinary fields. Polarization imaging is based on the study of vectorial properties of light and associated vectorial transformations resulting from light-matter interaction. The range of polarization imaging and its applications is so broad that it is very challenging to accommodate all relevant concepts and applications in a single literature. This review article is an attempt in this direction. This paper presents a concise review of polarization imaging from fundamental to advanced level, covering the essential elements, such as historical development, theoretical concepts, and experimental aspects of polarization imaging, followed by a brief introduction to traditional and modern polarization imaging instruments. This review article aims to provide a reference text for readers from various research backgrounds interested in polarization imaging.

1. Introduction

Polarization imaging is a cornerstone in imaging technology encompassing a broad range of applications, from optical microscopy to the study of giant objects in astronomy. Propagation of light through a medium exhibits notable changes in its inherent characteristics, i.e., intensity, phase, wavelength, polarization, etc. Conventional imaging sensors are primarily sensitive to the intensity and wavelength of light, and therefore, the initial development of imaging instruments evolved around the intensity and wavelength of light only. However, phase and polarization are crucial characteristics of light, which can be exploited to obtain the essential structural properties of sophisticated objects beyond the intensity and wavelength-dependent information. Unlike other light properties, the polarization of light interprets the vectorial characteristics of light waves. It provides a non-invasive pathway to study the crucial microstructural features of sophisticated objects. However, studying polarization and its interaction with materials is not straightforward; it requires advanced theoretical, experimental, and computational techniques. With the development of imaging technology over the years, the application of polarization information in imaging technology has been integrated into spatial, spectral, and structural information of the target object, which can not only provide vital information about the target object but also contribute to improving the image acquisition properties of an imaging system. In recent years, polarization imaging has shown potential application prospects in various fields, such as remote sensing [1,2], astrophysics [3,4], computational imaging [5–7], biomedical sciences [8–10], and other industrial domains [11,12]. Due to its interdisciplinary applicability and potential characteristics, polarization optics has always been an interesting research domain. Indeed, several excellent textbooks and review articles are dedicated to polarization optics [13–16]. However, the range of polarization optics is so broad that it is challenging to accommodate all the concepts and applications in a single piece of literature. Moreover, the complicated treatment of the concepts and polarization imaging techniques can make it difficult to understand and tedious to some readers, especially from non-optic backgrounds. Another notable issue in such literature is the inconsistency in scientific notations and terminology, which makes it tedious for the researchers to connect different associated topics in polarization imaging. Therefore, a review article on polarization optics and imaging techniques can help disseminate the advances in polarization imaging to a broader range of researchers from any background.

This paper concisely reviews polarization imaging from the fundamental to the advanced level. This review article is organized into seven sections, and each section contributes to the consistent treatment and consolidation of essential concepts, techniques, and applications of polarization imaging. Section 1 briefly introduces polarization imaging from a general perspective, followed by Section 2, which is dedicated to the evolution of polarization optics from the earliest development to the most recent advances in polarization imaging. Section 3 deals with the theoretical background of polarization optics and discusses the principles and mathematical formalism of robust polarization imaging

E-mail address: vipin.tiwari@ut.ee.

https://doi.org/10.1016/j.jqsrt.2025.109427
Received 2 August 2024; Received in revised form 30 January 2025; Accepted 6 March 2025
Available online 15 March 2025

techniques, i.e., Jones matrix calculus and Stokes-Mueller calculus. The experimental aspects of polarization imaging techniques, related notable studies, and results, along with the practical steps for their implementation, are discussed in Section 4. Section 5 provides a brief description of the essential polarization optical elements (polarizers, retarders, etc.), modern polarization instruments, such as four-polarization cameras, Liquid Crystal-Spatial Light Modulators (LC-SLM), etc., followed by the most recent frontiers in polarization optics, i.e., polarization-sensitive metasurfaces are mentioned briefly. In the final section, a summary, challenges, and future scopes are discussed in the concluding remarks. A pictorial representation of the structure of the review article is illustrated in Fig. 1.

2. History and development

Polarization is abundant in nature and can be observed through various optical phenomena, such as scattering, reflection, refraction, interference, etc. The first scientific study on polarization observation was reported four centuries back. Polarization was first observed by Erasmus Bartholinus [17] during his experiment on calcite crystal in the form of double refraction, followed by Christian Huygens [18]. In 1808, Louis Malus discovered the polarization of light by reflection and mathematically interpreted the intensity distribution of light after passing through linear polarizers, known as Malus's law [19]. Later, David Brewster made a crucial contribution to polarization optics and found the relationship between refractive index and angle of polarization (Brewster's angle) [20]. In 1816, Fresnel and Arago investigated the interference of polarized light and postulated the famous Fresnel-Arago laws [21]. In subsequent years, studies on polarization phenomena, such as polarization in scattering [22], optical activity [23], and photo-polarimetry [24], were reported, and novel polarization-sensitive optical devices, such as the Nicol prisms [25], sheet polarizers [26], etc., were invented. For more details, readers are directed to [27].

In the context of polarization imaging, the first mathematical formulation for defining the polarization state of an optical beam was given by George Gabriel Stokes in terms of four measurable quantities by measuring the intensity of light, known as Stokes Polarization Parameters (SPPs) [28,29]. The Stokes vector consists of a set of four quantities that are measured in terms of intensity and describe the polarization of light. The Poincare sphere, conceived by Henri Poincare, is a geometrical approach for studying polarization state [30]. In 1943, another technique, known as Mueller matrix calculus, was proposed for studying the interaction of polarized light with an anisotropic medium, which can change its polarization state [31]. In Mueller matrix calculus, the optical device is described as a matrix of order 4×4, light intensity measurements. A few years later, R. Clark Jones proposed a robust polarimetric technique in a coherent framework to retrieve the phase and polarization information of an anisotropic medium, known as Jones matrix calculus [32–35]. In Jones calculus, the incident light is described by the Jones vector, and the optical device is defined by its Jones matrix. The resultant polarization change is calculated by multiplying the Jones vector by the corresponding Jones matrix. The Jones and Mueller calculus is the most essential tool for studying different optical properties based on polarization state modulation.

Over the past few decades, a remarkable boom has been noticed in polarization imaging technology. The notable advancements are the integration of polarization in holography [36–39] and microscopy [40–42]. Polarization-resolved microscopy has improved the imaging capabilities of existing microscopic systems up to several orders and also played a crucial role in the development of recent state-of-art microscopic techniques, such as Stimulated Emission Depletion (STED) [43], Stochastic Optical Reconstruction Microscopy (STORM) [44]. More recently, metasurface-enabled polarization imaging has significantly enhanced its efficacy and feasibility in various applications [45]. Readers interested in more comprehensive details on the traditional and modern developments in polarization imaging in different fields may refer to [2,8–10,13,16,46–49]. Fig. 2 represents the overview of significant milestones in polarization imaging over the years.

3. Theoretical concepts

Polarization of light can be defined as the vectorial distribution of its

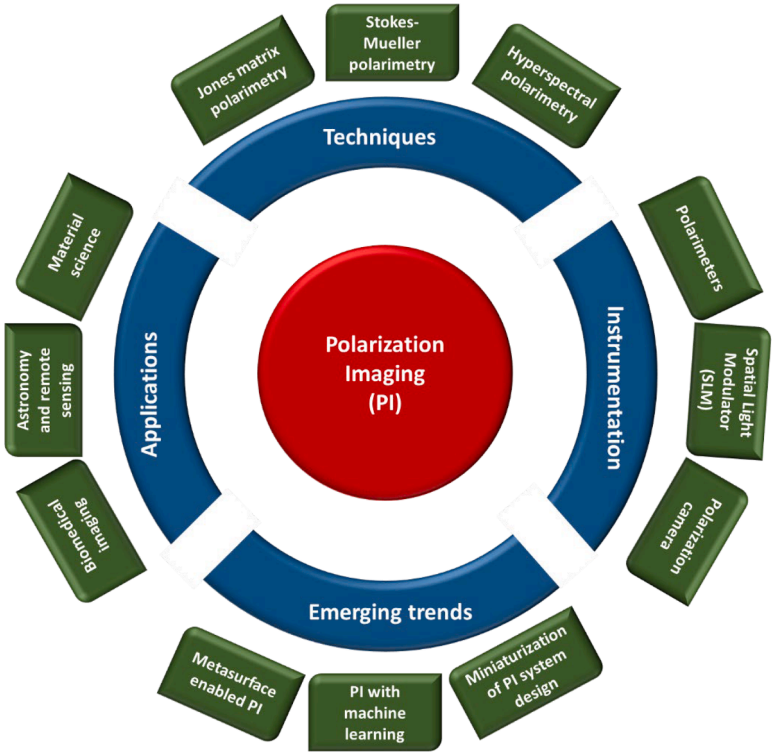

Fig. 1. Structure of the review article. Polarization imaging: Techniques, instrumentation, applications, and emerging trends.

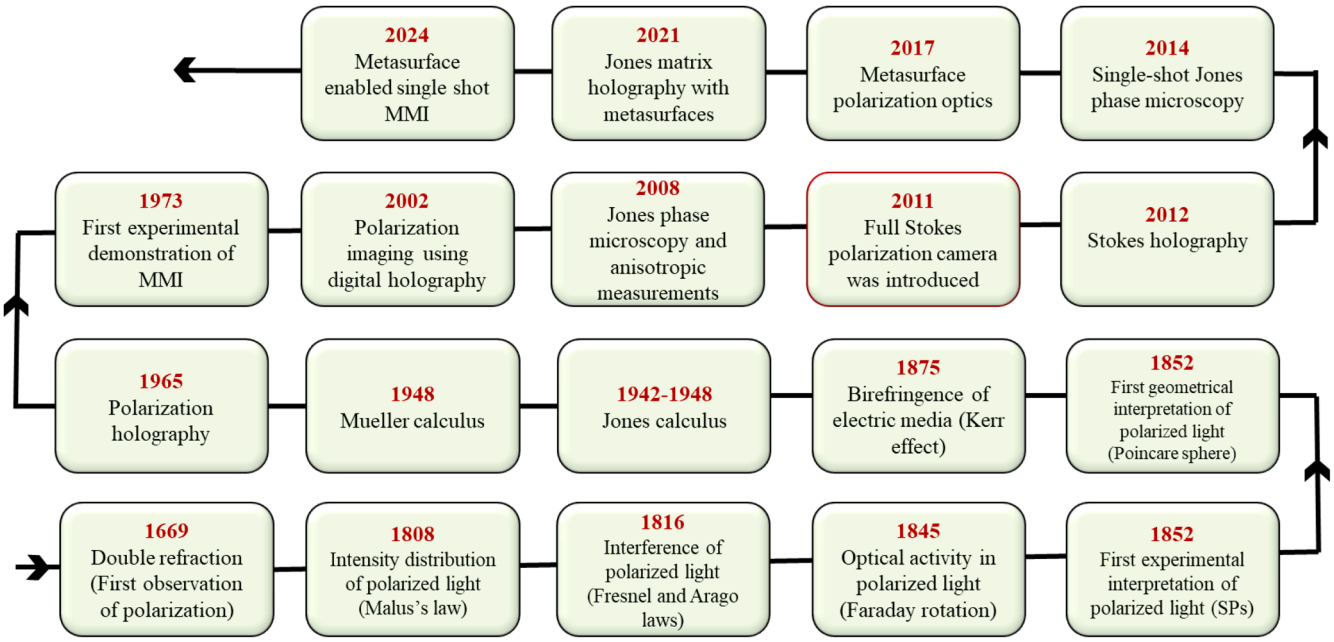

Fig. 2. Roadmap to significant milestones in Polarization imaging (in chronological order).

electric field components. Based on the relative oscillations of the electric field component of light, different states of polarization (SOP) are defined. Mostly, these oscillations are distributed randomly (in no particular direction) in natural light; hence, natural light is un-polarized. However, if a specific direction of such oscillations is filtered out by some means, the resultant light is termed polarized light to that particular direction. For example, if these oscillations are oriented horizontally, they are called horizontally polarized light with SOP horizontal 'H.' Similarly, other main SOPs can be defined based on the relative oscillations of electric field oscillations, viz., vertically polarized (V), diagonally, i.e., $+45^{\circ}$ polarized (P), anti-diagonally, i.e., -45° polarized (M), follows a circular path with clock-wise direction, i.e., right circularly polarized (R), and follows a circular path with anti-clockwise direction, i.e., left circularly polarized (L) respectively.

Studying the polarization of light requires a concrete theoretical framework to study the polarization of light and its interaction with different types of materials. Jones matrices, Stokes parameters, and Mueller matrices are essential theoretical concepts that must be interpreted to understand polarization imaging.

3.1. Jones matrix calculus

Jones matrix calculus is a rigorous tool for interpreting the polarization states of light in a coherent framework. In Jones calculus, the SOP of light is described as a two- dimensional complex-valued vector, known as the Jones vector. In the context of light-matter interaction, the product of the Jones vector of the input light with the Jones matrix yields the output polarization states of light after interacting with the object.

Following the plane wave solution of Maxwell's equations, the electric field vector of a plane wave is given as

$$E(z,t) = \begin{pmatrix} E_x e^{i\phi_x} \\ E_y e^{i\phi_y} \end{pmatrix} e^{i(\omega t - kz)} \tag{1}$$

The matrix of order (2×1) in Eq. (1) governs the electric field propagation of light and is known as the 'Jones vector.' Different values of field amplitude ($E_x and E_y$) and relative phase ($\phi = \phi_y - \phi_x$) yield different Jones vectors, which dictates different polarization states of light.

The polarization modulation of light after interacting with material interfaces can be described by measuring the Jones vector transformations. These linear transformations are valid (at least) for the imaging systems under the realm of linear optics. Mathematically, the input and output electric field components ($E_i and E_o$) are connected through an operator ($\boldsymbol{J}$) as

$$E_o = \boldsymbol{J}\, E_i \tag{2}$$

$$\boldsymbol{J} = \begin{pmatrix} J_{xx} & J_{xy} \\ J_{yx} & J_{yy} \end{pmatrix} \tag{3}$$

Where, $\boldsymbol{J}$ is a matrix of order 2×2, is defined as Jones matrix. Intuitively, Jones matrix ($\boldsymbol{J}$) consists of four complex entities, having the ability to manipulate the polarization by either attenuating the incident polarization or retarding the phase of light. However, Jones matrices calculus is primarily applicable for phase-driven polarization measurements and thus cannot be adapted as a versatile polarimetric approach, explicitly for imaging with partially polarized light. Moreover, the image sensors cannot measure the electric field directly in practice. Instead, they measure the intensity, i.e., the modulus square of the electric field. Stokes-Mueller calculus is another crucial polarimetric technique, depicting an extended description of polarization with intensity measurements.

3.2. Stokes-Mueller matrix calculus

Stokes polarization parameters (SPPs) are the first observable manifestation of partially polarized light. Unlike Jones matrices, SPPs offer a broader range of applications as these can be measured for partially and unpolarized light. SPPs are defined as four intensity observables, which can be measured by using different intensity combinations of light and can be written as

$$S = \begin{pmatrix} S_0 & S_1 & S_2 & S_3 \end{pmatrix}^T \tag{4}$$

Four SPPs are defined as

$$I = S_0 = I_H + I_V \tag{5}$$

$$Q = S_1 = I_H - I_V \tag{6}$$

$$U = S_2 = I_P - I_M \tag{7}$$

$$V = S_3 = I_R - I_L \tag{8}$$

From an experimental perspective, S_0 represents the total intensity (S_0) of light. The other three SPPs, i.e., S_1, S_2, *and* S_3, share intensity quotient corresponding to SOPs H, V, P, M, R, and L, i.e., I_H, I_V, I_P, I_M, I_R, and I_L respectively.

SPPs can be written in terms of electric field components as

$$S_0 = E_x E_x^* + E_y E_y^* \tag{9}$$

$$S_1 = E_x E_x^* - E_y E_y^* \tag{10}$$

$$S_2 = E_x E_y^* + E_y E_x^* \tag{11}$$

$$S_3 = i\left(E_x E_y^* - E_y E_x^*\right) \tag{12}$$

Further, SPPs are directly linked to the degree of polarization (DOP) of light as

$$DOP = \frac{\sqrt{S_1^2 + S_2^2 + S_3^2}}{S_0} \tag{13}$$

The value of *DOP* decides the proficiency of polarized light. For instance, *DOP*=1 refers to completely polarized light, *DOP*=0 corresponds to unpolarized light, and $0 < DOP < 1$ depicts light to be partially polarized.

Taking an analogy from Jones matrix calculus, SPPs form the basis for treating the optical system with partially or unpolarized light. However, the linear transformation of the input Stokes vector to the output Stokes vector can be carried out by using a generalized operator (**M**) as

$$S_o = \boldsymbol{M}.S_i \tag{14}$$

$$M = \begin{pmatrix} M_{11} & M_{12} & M_{13} & M_{14} \\ M_{21} & M_{22} & M_{23} & M_{24} \\ M_{31} & M_{32} & M_{33} & M_{34} \\ M_{41} & M_{42} & M_{43} & M_{44} \end{pmatrix} \tag{15}$$

Where $\boldsymbol{M}$ is a matrix of order 4 × 4, is defined as Mueller matrix. Mueller matrix calculus is an eminent matrix algebraic method to study the polarization characteristics of a medium, especially a depolarizing medium. Unlike the Jones matrix, Stokes-Mueller matrix calculus can be applied to any type of light source (coherent or incoherent) and sample (depolarizing), providing a more versatile polarimetric approach. The Jones vectors and Stokes vectors for different SOPs are summarized in Table 1.

3.3. Jones matrix and Mueller matrix transformation

The above discussion shows that Jones matrix calculus cannot be applied to partially polarized light. On the other hand, Stokes-Mueller calculus is preferred for partially polarized light, but its efficacy is questionable for phase measurements. Therefore, both these polarimetric techniques are equally important for polarimetric measurements. Fortunately, every Jones matrix has its Mueller matrix analog, and its elements can be defined as [50]

$$M_{ij} = \frac{1}{2} Tr\left(\boldsymbol{J}\sigma_j \boldsymbol{J}^{\dagger}\sigma_i\right) \tag{16}$$

Where, M_{ij} ($i, j = 1$ to 4) is the element of Mueller matrix (**M**) (i^{th} row and j^{th} column) corresponding to Jones matrix (**J**). σ_i is i^{th} Pauli matrix in polarization optics, defined as

$$\sigma_1 = \begin{pmatrix} 1 & 0 \\ 0 & 1 \end{pmatrix}, \sigma_2 = \begin{pmatrix} 1 & 0 \\ 0 & -1 \end{pmatrix}, \sigma_3 = \begin{pmatrix} 0 & 1 \\ 1 & 0 \end{pmatrix}, \sigma_4 = \begin{pmatrix} 0 & -i \\ i & 0 \end{pmatrix}, \tag{17}$$

However, inverse transformation (Mueller matrix to Jones matrix transformation) is not universal, i.e., only some (not all) Mueller matrix have corresponding Jones matrix. Mueller matrices with an equivalent Jones matrix can only be converted to a Jones matrix up to an overall phase. These transformations are not feasible for depolarizing Mueller matrices.

3.4. The Poincare sphere

In the Poincare sphere method, all SOPs can be visualized as residing on the surface of a sphere, i.e., the Poincare sphere. This method is based on the projection of different normalized SPPs at different spatial coordinates of the surface of the Poincare sphere, which represent the spatially varying SOPs. The normalized SPPs can be denoted as the spatial coordinates of a point on the Poincare sphere. The locus of SPPs depends on two geometrical parameters, i.e., azimuth angle (α) and ellipticity (β) as

$$\alpha = \frac{1}{2}\ arctan\left(\frac{S_2}{S_1}\right) \tag{18}$$

$$\beta = \frac{1}{2}\ arctan\left(\frac{S_3}{\sqrt{S_1^2 + S_2^2}}\right) \tag{19}$$

Points on the surface of the Poincare sphere designate fully polarized light, whereas a point on the origin of the Poincare sphere represents unpolarized light. The points on poles, equator, and other locations of the surface of the Poincare sphere indicate circularly polarized, linearly polarized, and elliptically polarized, respectively. Orthogonal polarizations on the Poincare sphere are given by polarization states whose Stokes vectors are diametrically opposite. A complete description of the Poincare sphere and different SOPs is shown in Fig. 3.

Table 1
Jones vector and Stokes vectors for different polarization states of light.

S. no.	Polarization state	Normalized Jones vector	Stokes vector
1	Horizontal (H)	$\begin{pmatrix}1\\0\end{pmatrix}$	$(1\ \ 1\ \ 0\ \ 0)^T$
2	Vertical (V)	$\begin{pmatrix}0\\1\end{pmatrix}$	$(1\ \ -1\ \ 0\ \ 0)^T$
3	+45° (P)	$\frac{1}{\sqrt{2}}\begin{pmatrix}1\\1\end{pmatrix}$	$(1\ \ 0\ \ 1\ \ 0)^T$
4	−45° (M)	$\frac{1}{\sqrt{2}}\begin{pmatrix}1\\-1\end{pmatrix}$	$(1\ \ 0\ \ -1\ \ 0)^T$
5	Right circular (R)	$\frac{1}{\sqrt{2}}\begin{pmatrix}1\\-i\end{pmatrix}$	$(1\ \ 0\ \ 0\ \ 1)^T$
6	Left circular (L)	$\frac{1}{\sqrt{2}}\begin{pmatrix}1\\i\end{pmatrix}$	$(1\ \ 0\ \ 0\ \ -1)^T$

4. Experimental aspects

4.1. Basic components of polarization imaging system

Familiarizing with the structure and utilization of fundamental Polarization Optical Elements (POE) is recommended to understand polarization imaging techniques. POEs are the essential components of polarization imaging systems employed to generate, analyze, and manipulate the SOP of light. Based on different applications, POEs are classified into four types, *viz.*, attenuators (linear polarizers), retarders, rotators, and depolarizers. Polarizers transmit light at a fixed polarization state along its transmission axis. Based on their construction and working mechanisms, they are generally categorized into three major types (absorption polarizers, reflection polarizers, and refraction polarizers). Despite the optimized SOP modification, polarizers cut off some of the total output intensity following Malus's law. Retarders are another type of POEs, which modulate the SOP of light by introducing a

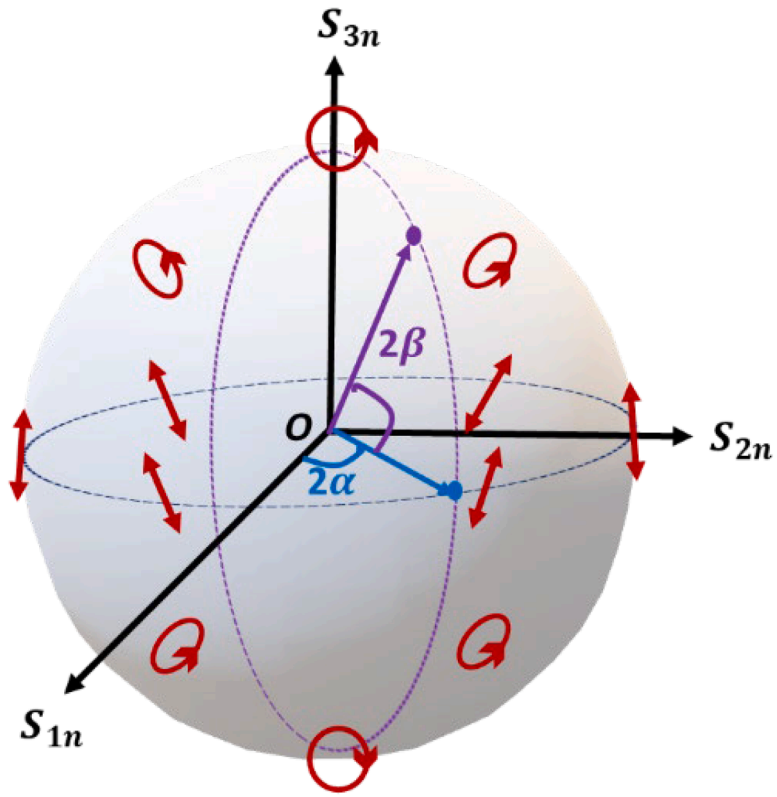

Fig. 3. Poincare sphere representation of polarization states of light. α: azimuth angle, β: ellipticity, and $S_{1n}S_{2n}S_{3n}$ are normalized Stokes vectors. Red color geometries represent different SOPs of light at different regions of Poincare sphere.

specific phase difference between the orthogonal field components of incident light. Birefringent retarders, variable retarders, and achromatic retarders are the primary optical retarders. From the experimental point of view, Half-Wave Plates (HWP) and Quarter-Wave Plates (QWPs) are the most commonly used retarders in polarization optics. Unlike polarizers, retarders rotate the SOP of light and can modulate the SOP of input light without compromising its intensity. Another class of POEs are optical rotators, which modulate SOP using the optical activity of input light. The optical activity of a crystal can be described in terms of LCP and RCP light and the corresponding refractive indices. Therefore, optical rotators are crucial POEs to determine light's handedness (helicity) after passing through an object. Faraday rotator is an example of an optical rotator commonly used in polarimetry. The fourth type of POE is depolarizer. A depolarizer reduces the degree of polarization (DOP) and, therefore, can also modulate the SOP of light. For instance, scattering media (turbid media, fog, biological tissues, etc.) can manipulate the DOP of input light and, hence, work as a depolarizer.

4.2. Jones matrix imaging

Experimental measurement of the Jones matrix is not straightforward as it contains complex-field information. The principles of holography and interferometry are adapted to record an object's complex-field (amplitude and phase) information. Fig. 4(a) illustrates a generalized Jones matrix imaging layout. Jones matrix imaging requires multiple shots to record the Jones matrix of an object. For instance, in double shot Jones matrix imaging, the sample is first illuminated with $+45^\circ$ in one shot followed by -45° polarized input light in the second shot. Following Eqs. (2) and (3), the output electric field components for these cases (two shots) can be written as

$$\begin{pmatrix} E_{px} \\ E_{py} \end{pmatrix} = \begin{pmatrix} J_{xx} & J_{xy} \\ J_{yx} & J_{yy} \end{pmatrix} \begin{pmatrix} 1 \\ 1 \end{pmatrix} \tag{20}$$

$$\begin{pmatrix} E_{mx} \\ E_{my} \end{pmatrix} = \begin{pmatrix} J_{xx} & J_{xy} \\ J_{yx} & J_{yy} \end{pmatrix} \begin{pmatrix} 1 \\ -1 \end{pmatrix} \tag{21}$$

The Jones matrix components of can be easily extracted by solving Eqs. (20, 21) as

$$J_{xx} = \frac{1}{2}\left[E_{px} + E_{mx}\right] \tag{22}$$

$$J_{xy} = \frac{1}{2}\left[E_{px} - E_{mx}\right] \tag{23}$$

$$J_{yx} = \frac{1}{2}\left[E_{py} + E_{my}\right] \tag{24}$$

$$J_{yy} = \frac{1}{2}\left[E_{py} - E_{my}\right] \tag{25}$$

Jones Matrix Imaging (JMI) demands robust and compact interferometric systems to retrieve the amplitude and phase response of the target object simultaneously. The earlier reported studies on JMI required multiple shots to record complex field information. Some of the notable multiple-shot JMI techniques are Jones phase microscopy [51], polarization holographic microscopy [52], and polarization-sensitive digital holographic microscopy [53]. Multiple-shot JMI is unsuitable for real-time imaging applications, such as dynamic samples. In recent years, a few studies on single-shot JMI have been reported [49,54–57]. *Sreelal* et al. proposed Jones matrix microscopy from a single-shot intensity measurement and experimentally determined the Jones matrix components of liquid crystal droplet [54]. *Chang* et al. proposed a single-shot Jones matrix measurement method using an ultrafast laser and experimentally demonstrated it for different isotropic and anisotropic samples [58]. The measured Jones matrix components of the LC cell (aromatic lipid thermotropic liquid crystalline cell, thickness =10 μm at 4 V applied voltage) are shown in Fig. 5. The study's results demonstrate the quantitative measurement of Jones matrix components

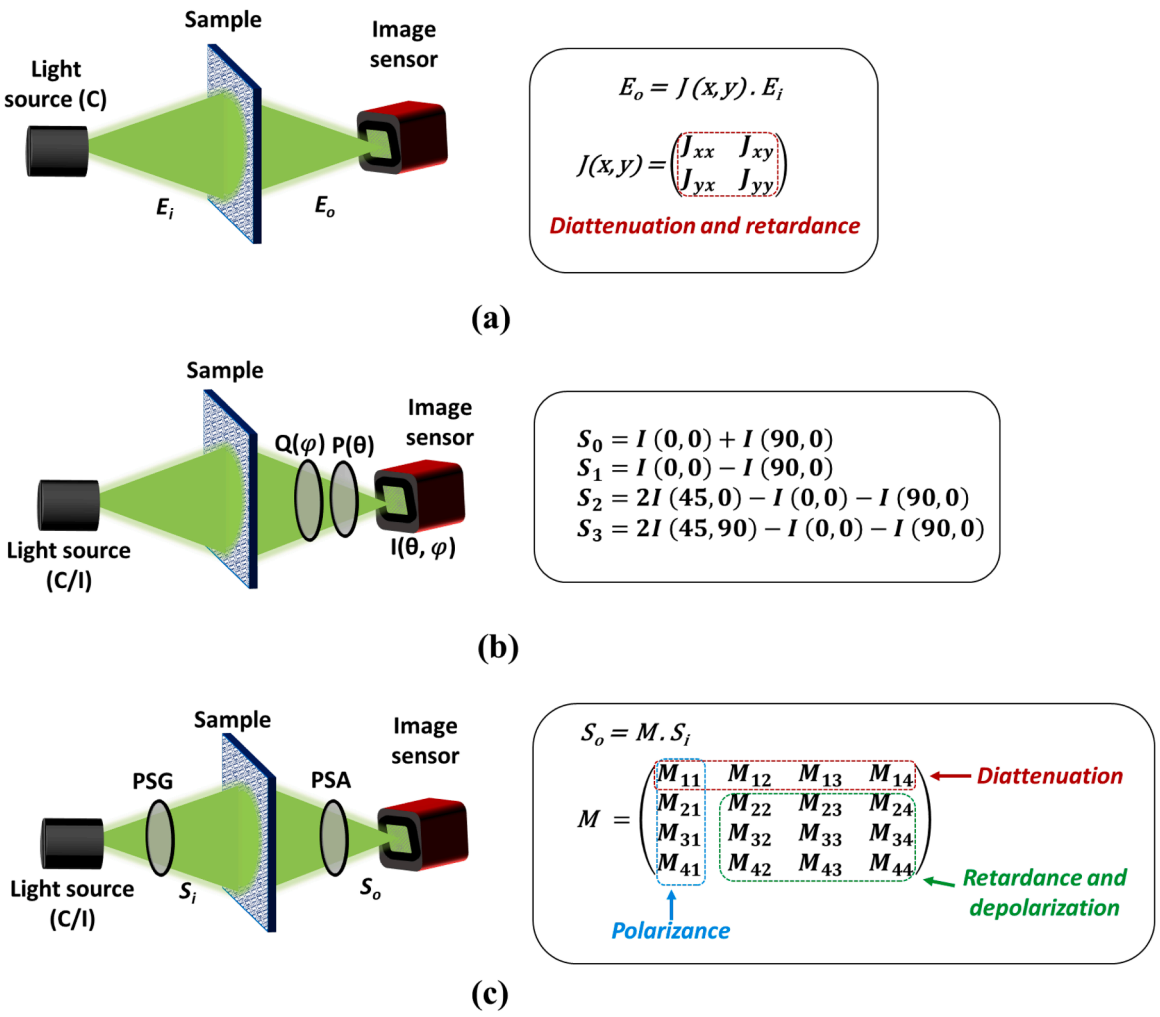

Fig. 4. Polarization imaging techniques. **(a)** Jones matrix imaging, **(b)** Stokes polarimetry, **(c)** Mueller matrix imaging. (C: coherent, I: incoherent, S_i: Stokes parameter (input), S_o: Stokes parameter (output), J: Jones matrix, Q (φ): Quarter wave plate at angle φ, P (θ): Polarizer at angle θ, M: Mueller matrix, PSG: Polarization State generator, PSA: Polarization State Analyzer).

with high spatial resolution and also suggest possibilities to achieve real-time Jones matrix measurement in ultrafast processes. In another study, *Yang* et al. measured the spatially-resolved Jones matrix of biological samples in a single shot [57]. Besides, *Liu* et al. reported a real-time compact inline holographic microscopic technique to measure the real-time Jones matrix synthesis [59]. More recently, metasurface-enabled Jones matrix holography has been proposed and experimentally demonstrated for the polarization-modulating computer-generated holograms for customized polarization and birefringence control [60].

4.3. Stokes polarimetry

Stokes polarimetry is the technique for recording the SPPs of the sample. The experimental measurements of SPPs require multiple recordings. In general, the Stokes polarimetric techniques can be divided into two categories, i.e., non-simultaneous Stokes polarimetry and simultaneous Stokes polarimetry. Non-simultaneous Stokes polarimetric methods are conventional and utilize rotating polarizers and phase retarders (wave plates) to measure SPPs from multiple recordings at different times. The SPPs can be experimentally measured using a typical rotatory Stokes-polarimeter, which consists of a phase retarder (preferably QWP) followed by a linear polarizer, as shown in Fig. 4(b). Phase retarder is referred to a phase-shifting optical element, which can advance or retard the relative phase of field components ($E_x and E_y$) by φ /2 and the linear polarizer transmits the optical field along its transmission axis (at angle θ) only.

Following Eqs. (9-12), the all four SPPs can be written in single intensity equation

$$I(\theta,\phi) = \frac{1}{2}[S_0 + S_1\cos 2\theta + S_2\cos\varphi\ \sin 2\theta + S_3\sin\varphi\ \sin 2\theta] \quad (26)$$

For SPPs, four intensity configurations, i.e., intensities at four different rotation angles of retarder (φ) and linear polarizer (θ) are measured as in order $I(0, 0)$, $I(45, 0)$, $I(90, 0)$, $I(45, 90)$ respectively. SPPs can be determined by using following equations:

$$S_0 = I\ (0,\ 0) + I\ (90,\ 0) \quad (27)$$

$$S_1 = I\ (0,\ 0) - I\ (90,\ 0) \quad (28)$$

$$S_2 = 2I\ (45,\ 0) - I\ (0,\ 0) - I\ (90,\ 0) \quad (29)$$

$$S_3 = 2I\ (45,\ 90) - I\ (0,\ 0) - I\ (90,\ 0) \quad (30)$$

Rotatory Stokes polarimeters [61] are simple in structure and low cost, but they require multiple recordings at different times, which makes them inefficient for real-time polarimetry. Another example of a non-simultaneous Stokes polarimeter is the electronically controlled Stokes polarimeter [62–64], which replaced traditional waveplates with electrically addressed phase delay devices, such as LC-SLM [62],

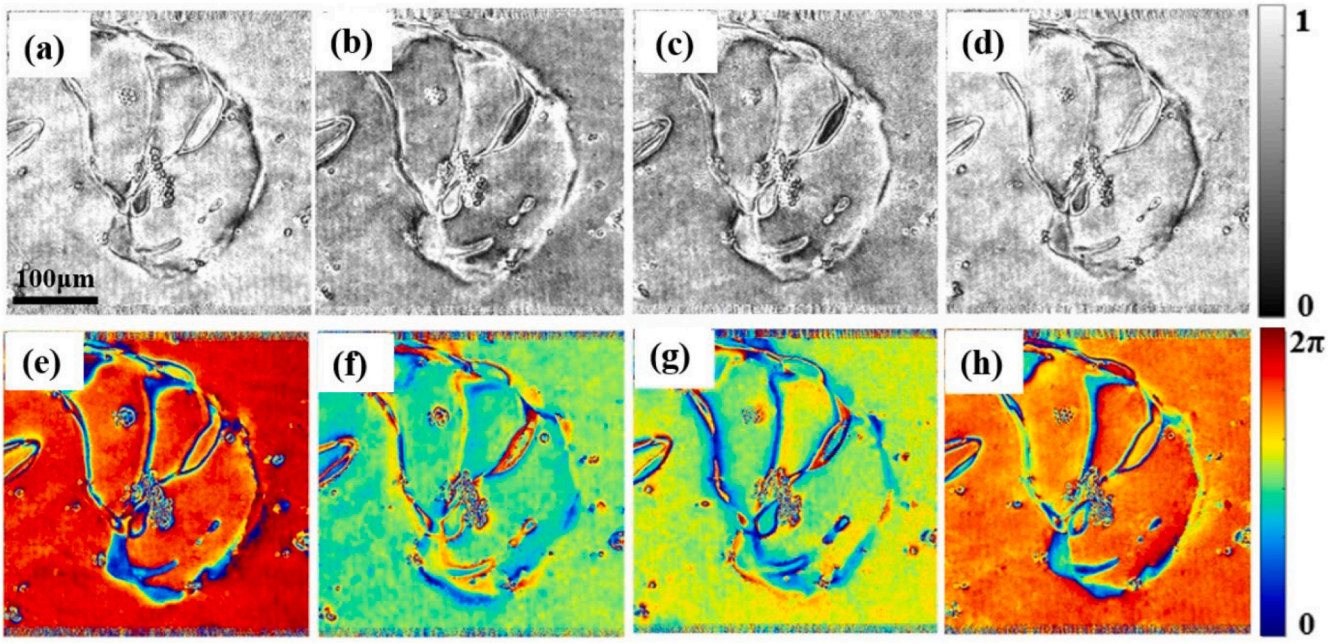

Fig. 5. Single-shot Jones matrix imaging using an ultrafast laser. **(a-d)** amplitude distributions of Jones matrix components. **(e-h)** phase distribution of Jones matrix components of aromatic lipid thermotropic liquid crystalline cell, thickness =10 μm at 4 V applied voltage). (*adapted from* [58] *under Creative Commons Attribution license 4.0*).

photo-elastic modulators (PEMs) [64]. This replacement provides these Stokes polarimeters with a dynamic phase delay but also introduces complexity in its design.

On the other hand, simultaneous Stokes polarimetry also has categories, i.e., amplitude and focal plane division. In the division of amplitude Stokes polarimetry, incident light is divided into multiple channels through a polarization beam splitter or Wollaston prism to simultaneously record multiple SOP intensity information. *Azzam* et al. designed the first division of the amplitude Stokes polarimeter using a Polarization Beam Splitter (PBS) and four charge-coupled devices (CCDs) [65], followed by subsequent modifications in design [66–68]. The second category, simultaneous Stokes polarimetry, i.e., division of focal plane works on the principle of division of Focal Plane Array (FPA), where different micro-polarizer polarization orientations are integrated into FPA [69]. It leverages to record four linear SOPs of light in a single shot, which makes it a time-efficient approach with the compact and stable design of the Polarization camera [70].

4.4. Mueller matrix imaging

The Mueller matrix of the target sample can be measured with a Mueller-Matrix Imaging Polarimeter (MMIP). A typical MMIP has two main components, i.e., Polarization State Generator (PSG) and Polarization State Analyzer (PSA), as shown in Fig. 4(c). PSG and PSA consist of a set of linear polarizers and phase retarders inserted before and after the sample to generate different SOPs of light. Various input and output SOP combinations of light corresponding to input and output configurations of PSG and PSA are summarized in Table 2.

Following Eq. (15), the Mueller matrix of the target object can be measured by recording different SOP combinations as follows:

$$M = \begin{pmatrix} I_{HH}+I_{HV}+I_{VH}+I_{VV} & I_{HH}+I_{HV}-I_{VH}-I_{VV} & I_{PH}+I_{PV}-I_{MH}-I_{MV} & I_{RH}+I_{RV}-I_{LH}-I_{LV} \\ I_{HH}-I_{HV}+I_{VH}-I_{VV} & I_{HH}-I_{HV}-I_{VH}+I_{VV} & I_{PH}-I_{PV}-I_{MH}+I_{MV} & I_{RH}-I_{RV}-I_{LH}+I_{LV} \\ I_{HP}+I_{HM}-I_{VP}-I_{VM} & I_{HP}-I_{HM}-I_{VP}+I_{VM} & I_{PP}-I_{PM}-I_{MP}+I_{MM} & I_{RP}-I_{RM}-I_{LP}+I_{LM} \\ I_{HR}-I_{HL}+I_{VR}-I_{VL} & I_{HR}-I_{HL}-I_{VR}+I_{VL} & I_{PR}-I_{PL}-I_{MR}+I_{ML} & I_{RR}-I_{RL}-I_{LR}+I_{LL} \end{pmatrix} \tag{31}$$

Table 2
Intensity measurements (SOP combinations) for Mueller matrix imaging.

SOP	H	V	P	M	R	L
H	I_{HH}	I_{HV}	I_{HP}	I_{HM}	I_{HR}	I_{HL}
V	I_{VH}	I_{VV}	I_{VP}	I_{VM}	I_{VR}	I_{VL}
P	I_{PH}	I_{PV}	I_{PP}	I_{PM}	I_{PR}	I_{PL}
M	I_{MH}	I_{MV}	I_{MP}	I_{MM}	I_{MR}	I_{ML}
R	I_{RH}	I_{RV}	I_{RP}	I_{RM}	I_{RR}	I_{RL}
L	I_{LH}	I_{LV}	I_{LP}	I_{LM}	I_{LR}	I_{LL}

The experimental measurement of the Mueller matrix using conventional MMIP is a time-consuming task as it requires at least 36 intensity measurements [72]. With the advancement of imaging technology, attempts have been made to reduce the number of recordings to measure the Mueller matrix. Some initial reported studies used the analytical approach, where 36 intensity measurements were reduced to 16 using the SOP conservation rule [73]. However, this approach introduces measurement errors as well. Further developments in MMI techniques introduced a snapshot Mueller matrix microscope, which utilized the idea of replacing conventional CCDs with the 4-polarization camera [74]. It reduced the required recordings but introduced some computational bottlenecks, such as pixel cross-talk and low-spatial resolution, while processing the four-polarization images. Furthermore, Mueller matrix optical scanning microscopy was introduced to address

the spatial resolution and computational issues in snapshot MMI. This technique integrates the conventional MMIP into the scanning laser microscopy design for the single and multiple-channel temporal and spectral Mueller matrix acquisition by scanning the target sample [75]. In the most recent developments in MMIP, metasurface-enabled compact and robust MMI is proposed, which enables the acquisition of all 16 intensity measurements of spatially varying Mueller matrix in a single shot [76].

The most prominent applications of MMI can be seen in biomedical imaging, where JMI is not that useful because of the high depolarizing characteristics of biological samples. Moreover, the Mueller matrix of a sample can be transformed into crucial anisotropic parameters, which are explicitly associated with specific microstructural features of the sample. Recently, *Sheng et al.* experimentally measured the Mueller matrices of anisotropic phantoms (silk sample and GRIN lens) and thoroughly investigated the connection between Mueller matrix transformation parameters and the structural characteristics of samples [71]. For demonstration, measured Mueller matrix images of silk phantom and GRIN lens are shown in Fig. 6, indicating a significant change in the Mueller matrix elements of both anisotropic samples. This variation in Mueller matrix elements signifies the samples' strong anisotropic and depolarizing characteristics.

It is noteworthy that JMI and Stokes-Mueller polarimetry are the most promising polarimetric techniques, but they have their own advantages and limitations. JMI is useful for extracting the phase information of a homogeneous medium, while the latter enables the complete polarization features of a depolarizing medium. JMI utilizes the Jones calculus to interpret the interaction of polarized light with the sample.

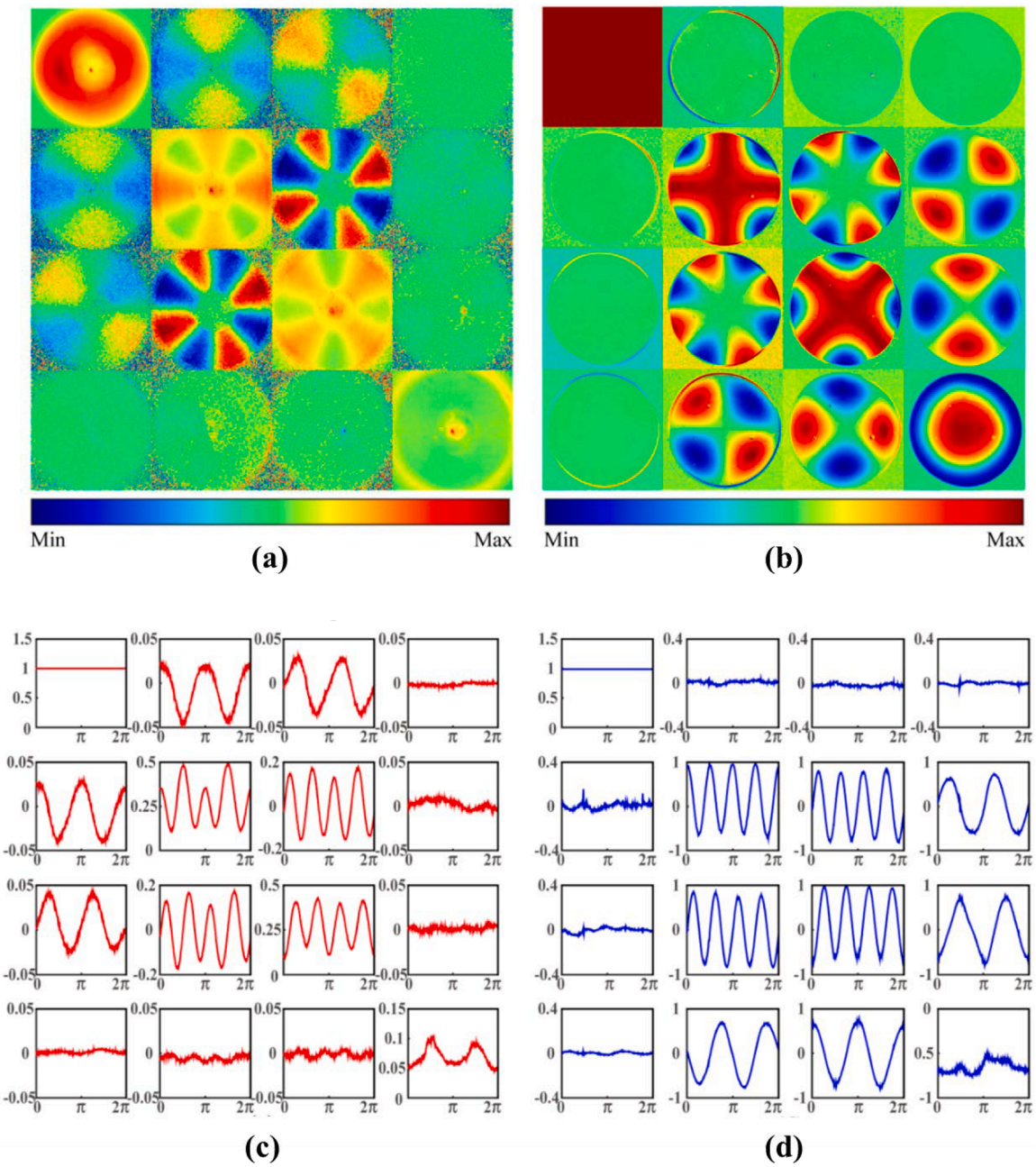

Fig. 6. Mueller matrix imaging of biological samples. **(a)** A 2D backscattering Mueller matrix image of silk phantom. **(b)** A 2D transmission Mueller matrix image of birefringent gradient-index (GRIN) lens. Azimuthal-dependent curves of the Mueller matrix elements for **(c)** the silk phantom and **(d)** the GRIN lens. (*adapted from* [71] *under Creative Commons Attribution license 4.0*).

JMI is helpful in the anisotropic characterization of LC devices, such as SLM, and the investigation of birefringent materials[12,77]. JMI is quick as it requires only one or two shots to record Jones matrix, and it can be directly decomposed into the anisotropic properties, such as diattenuation and retardance. Considering limitations, it is suitable for depolarizing samples only. This limits its applicability in tissue polarimetry due to depolarizing characteristics of biological samples. However, modern polarimetric techniques, such as polarization-sensitive optical coherence tomography (OCT), exploit the Jones matrix of samples for different biomedical applications [78,79]. On the other hand, MMI utilizes the Mueller matrix (combination of Stokes parameters) to manifest the interaction of light with a sample, including changes in polarization. Unlike JMI, MMI has no restrictions, such as the need for coherent sources and non-depolarizing samples, which makes it a more promising candidate in polarimetry with diverse applications. However, Mueller matrix measurement is time-consuming as multiple intensity measurements are required to measure the Mueller matrix, which can be considered a significant demerit of MMI. Recently, studies have been reported to address this problem by integrating optical metasurfaces in polarimetry, leading to single-shot Mueller matrix measurement [76,80,81]. Also, combined Jones-Stokes polarimetry is another emerging direction that can provide more comprehensive information about a sample by combining the strengths of both polarimetric techniques [82]. The qualitative comparison of both these polarimetric techniques is presented in Table 3.

4.5. Hyperspectral polarimetry

Hyperspectral polarimetry is a robust technique in polarization imaging that lies at the intersection of hyperspectral imaging and polarimetry. Hyperspectral imaging allows compressive recording of images of an object at different spectral bands of the electromagnetic spectrum. Combining conventional polarization imaging techniques with hyperspectral imaging can lead to a more advanced technique, i.e., hyperspectral polarimetry, which offers spectrally-resolved polarization image acquisition of the sample [83]. The multi-dimensional datacube (intensity, spectrum, and polarization) in hyperspectral polarimetry can be recorded using scanning or snapshot imaging techniques [84–88]. In recent years, hyperspectral polarimetry has been exploited in a broad range of applications, i.e., biomedical imaging [89,90], atmospheric sciences [91,92], astrophysics [93], remote-sensing [92,94,95], etc., due to its promising multidimensional (spatial, spectrum, polarization) imaging capabilities. However, traditional spectropolarimeters require a long acquisition time and high-level storage to record high-dimensional datacube. These challenges can be addressed through the compressive sensing technique, which shortens the acquisition time and storage in conventional spectropolarimeters [85,96]. Additional challenges in hyperspectral polarimetry are bulky imaging systems, high cost, complex data processing, etc., which limit its applicability in real-time imaging processes. Integrating recent breakthroughs, such as computational imaging, machine learning, and optical metasurfaces in traditional hyperspectral polarimetry, can address these challenges in hyperspectral polarimetry. Despite these challenges, hyperspectral polarimetry is a rapidly emerging field demonstrating potential applications in imaging technology. Some of the recent developments in this direction are [87,97,98].

Table 3
Comparison of Polarization imaging techniques.

S. No.	Parameters	Jones matrix imaging (JMI)	Stokes-Mueller polarimetry
1.	Light source	Coherent	Coherent or incoherent
2.	SOP of input light beam	Fully polarized	Unpolarized, partially or fully polarized
3.	Required recording	Complex-field (Intensity and phase)	Intensity only
4.	Minimum required shots	1	16
5.	Sample type	Anisotropic but non-depolarizing	Anisotropic and depolarizing
6.	Output characteristics of the sample	Diattenuation, retardance	Diattenuation, retardance, depolarization
7.	Potential applications	Quantitative phase microscopy, holography, Optical coherence tomography	Tissue polarimetry, astronomy, remote-sensing, etc.

5. Polarization instrumentation

5.1. Polarization-sensitive detectors

Conventional image sensors are sensitive to the intensity and wavelength of light and thus are constrained by limited imaging acquisition capabilities. To capture polarization-sensitive information with traditional cameras, a division of time approach is used, i.e., multiple images must be captured at the different orientations of a linear polarizer placed before the sensor. However, this is a time-consuming approach that doesn't meet the requirements of modern imaging applications. With the development of polarization imaging technology, polarization-sensitive image sensors have been developed. Polarization cameras can record the polarization-dependent information of the object and provide information based on the birefringence and surface properties of the object. However, the structure of the polarization camera is sophisticated as it requires the compact design of polarization filters. Polarization cameras work on the division of focal plane technique in which pixel-wise multidimensional wire-grid polarizers are used to record spatially varying polarization information [99,100]. The microgrid polarizers are arranged along four different linear SOPs of light and are sandwiched between a micro-lens array and photodiodes. A schematic of the structure of the polarization camera is shown in Fig. 7(a). This approach is time-efficient and can acquire polarization images of dynamic objects as well. On the other hand, one drawback of the polarization camera is that only linear polarization is accountable for using such sensors. For example, polarization cameras are capable of recording linear SPPs only. Circular polarization states must be measured simultaneously to measure full SPPs and Mueller matrices of the sample. In recent years, polarization cameras for full-Stokes polarimetry have been proposed and experimentally demonstrated [81,101,102]. However, the efficiency and accuracy of such devices are still need to be optimized.

5.2. Polarization modulators

The optimized polarization modulation is a critical requirement in polarimetry. A systematic change in SOP can mitigate the undesired effects, such as low signal-to-noise ratio (SNR), contrast infidelity, etc., in polarization-sensitive instruments. A controlled phase delay between two orthogonal SOPs typically introduces polarization modulation. Traditional polarization modulators utilized the concept of rotating wave-plates. For example, a HWP with (phase delay of π) and a QWP (phase delay of $\pi/2$) were used to modulate the linear polarization and circular polarization state of light during the early stage of polarimetry. Further, the advancement of LC technology opened new possibilities for realizing more sophisticated optical modulators with optimized polarization modulation capabilities.

LCs are essential to the polarization modulators' design due to their polarization-dependent birefringence and voltage tunability. An LC device can be manifested as a layer of LCs sandwiched between two substrates. Different orientations of LC cells provide unique characteristics to the LC device. In context to the scope of this review, two configurations, i.e., parallel-aligned nematic (PAN) and twisted-nematic (TN), are crucial as most of the polarization modulators are designed based on

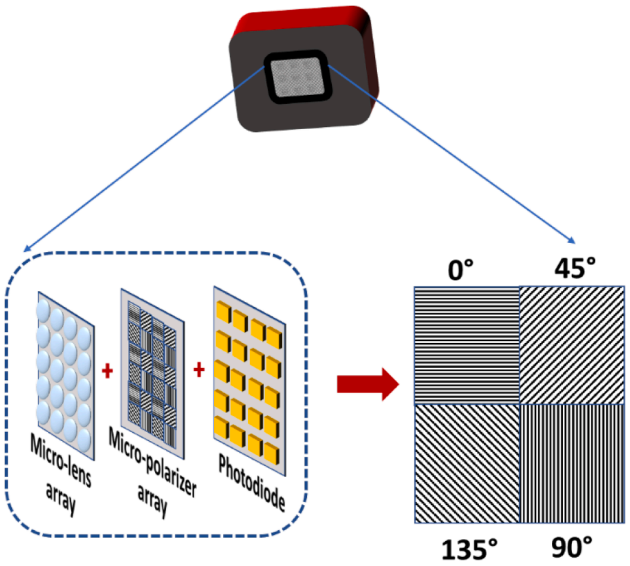

(a)

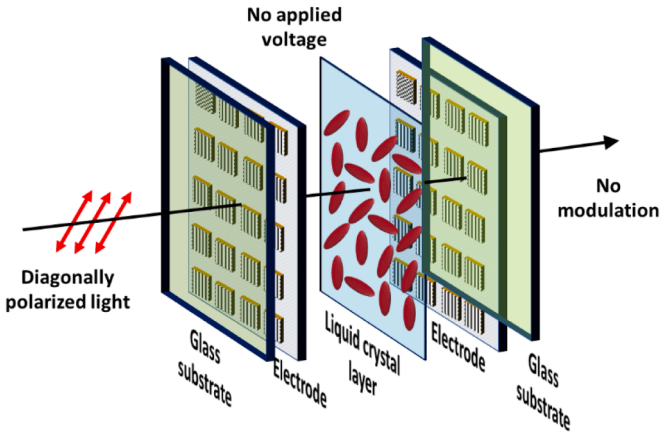

(b)

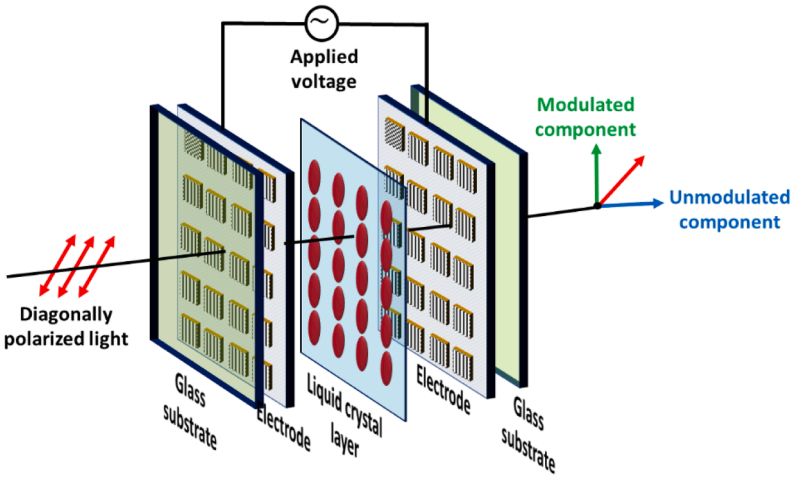

(c)

Fig. 7. Modern instruments in polarization imaging. **(a)** Polarization camera based on division of focal plane, **(b, c)** working principle of LC-SLM, **(b)** LC-SLM in the non-modulating state, **(c)** LC-SLM in the modulating state. [LC-SLM: Liquid crystal spatial light modulator].

these configurations. In PAN, the orientation of LC cells is parallel to the direction of the substrates. When an external voltage is applied, LCs rotate to align along the direction of the electric field. It results in a shift in the retardance of LC cells. On the other hand, LC cells are arranged in a specific helical structure in the TN configuration. Albeit, both LC configurations (PAN and TN) exhibit voltage dependent polarization modulation. In modern LC devices, such as LC-SLM, TN architecture is preferred due to slightly additional advantages, such as a better field of view.

LC-SLMs are modern electro-optical devices demonstrating excellent intensity, phase, and polarization modulation characteristics in diverse applications. SLMs work on the principle of LC, i.e., LCs tend to align along the direction of the applied external electric field. SLM's structure can be considered a typical alignment of LC molecules (nematic phase) sandwiched between transparent electrodes and glass substrates. The active matrix circuit is formed on the silicon substrate to control each pixel electrode using the individual electrical potential applied by semiconductor technology. The typical alignment of LC molecules of SLMs allows the change only along their director axis while the other orthogonal direction remains invariant. It results in optical anisotropy (phase retardation) due to SLM and is responsible for the phase shift at any location of the SLM display. The optimized phase shift for each pixel of the SLM is programmed as an 8-bit array (256 gray scales ranging from 0 to 255). Therefore, the typical anisotropic properties of SLM (phase shift and birefringence) can also be interpreted as a function of its gray scales. SLMs are programmed such that the orientation of LC molecules can be changed depending on their applied pixel voltage (gray scales). LC materials in SLMs depend on their optical and electrical anisotropic properties. LC-SLM shows an anisotropic nature due to the relative phase delay (birefringence) for the orthogonal polarization components of its LC array. In the normal state, when there is no pixel voltage applied and input light is not aligned along the active axis of SLM, the LC molecules are arranged in a random pattern and SLM shows no modulation characteristics. On the other hand, when pixel voltage (grayscale) is applied to the SLM, it provides an additional phase to the y-polarized light, whereas the x-component of light remains unaffected (Fig. 7(b, c)). SLMs offer a dynamic range of phase and polarization modulation characteristics, which have frequently been exploited in imaging systems in the last few decades [103]. Sometimes, SLMs are not ready-to-use optical devices as they might suffer from structural discrepancies, manufacturing defects, etc., affecting their optimized modulation capabilities. To overcome these issues, prior characterization studies are recommended before use [77,104–106]. Moreover, SLMs suffer from notable limitations such as limited pixel size (~microns), structural complexities, etc. These limitations of SLM constrain their utility in real imaging applications and encourage the development of polarization modulators that match advanced imaging requirements.

5.3. Polarization-sensitive metasurfaces

Over the past few years, metasurfaces have gained substantial interest in the research fraternity due to their prominent optical response-modulating features within subwavelength regimes. Metasurfaces exhibit a wide range of optical modulation capabilities across multiple information channels (intensity, phase, wavelength, polarization, etc.) of light using holographic multiplexing [107]. The polarization and phase modulation capabilities of metasurfaces have paved the way to achieve polarization imaging in the real-time domain. For instance, polarization-sensitive metasurfaces offer spatially varying polarization control of light by manipulating its birefringence [108]. Metasurfaces can be fabricated by tailoring geometric phases in the orthogonal basis of circular polarization states. For example, q-plates can generate optical beams carrying Orbital Angular Momentum (OAM) coupled with polarization handedness [109]. Different SOPs can be recorded simultaneously by projecting linearly and circularly polarized light using metasurfaces. Therefore, polarization-sensitive metasurfaces enable the acquisition of Stokes-Mueller polarimetry and Jones microscopy with minimal measurements using a compact experimental configuration. Recent studies suggest obtaining spatially varying polarization modulation using polarization-sensitive metasurfaces [110]. The optimized polarization control can be achieved by tuning the Jones and Mueller matrix of the optical system [60,76]. Fig. 8 shows the polarization imaging results obtained from conventional polarization imaging and a metasurface-enabled polarization camera [80,101]. It confirms that metasurface-enabled polarization imaging has certain merits over conventional polarization imaging systems, such as compact design and time-resolved polarimetry.

6. Applications

In the past few decades, polarization imaging has been exploited in a plethora of traditional multidisciplinary fields, i.e., atmospheric remote sensing, astronomy, biomedical imaging, holography, metrology, etc. However, recent breakthroughs, such as polarization-resolved microscopy, polarization-sensitive metasurfaces, etc., have pushed its applications to industrial domains as well. In recent years, polarization imaging has been employed in unconventional fields, i.e., advanced manufacturing [110], defense and surveillance [112], underwater imaging [113], etc. The potential applications of polarization imaging in some of these fields are discussed in subsequent sections.

6.1. Atmospheric remote sensing

Polarimetry is considered a robust technique in Atmospheric Remote Sensing (ARS), demonstrating exceptional imaging capabilities which are not possible in conventional imaging. Polarization-sensitive properties of scattered sunlight provide vital structural properties, such as shape, chemical composition, optical thickness, etc., of aerosol particles. Such polarization measurements are crucial for studying health issues due to aerosols by investigating atmospheric constituents' scattering and absorption properties. In the ARS domain, polarimetry is implemented using ground-based polarimetric instruments [114] and satellite instruments [115,116]. Some of the exemplary polarimetric instruments in ARS are the POLDER instrument [117], multi-angle spectro polarimeter imager (MSPI) [118], etc. More relevant details can be found in [2]. Fig. 9(a) demonstrates the spectrally-resolved polarization imaging for the sunlight region. The left image is the color image composited of three wavelengths, i.e., 565 nm, 670 nm, and 865 nm, and the right image is the corresponding Degree of Linear Polarization (DoLP) curve [119].

6.2. Astronomy

Polarization is an important phenomenon in astronomy. In astronomy, the direct applications of polarization imaging can be seen as polarimetric instrumentation, which detects polarization-discriminated signals from celestial bodies [3,120]. Generally, light from the astronomical objects is polarized due to their spherical asymmetry. For instance, the sensitive tendency of magnetic fields to split lines enables the probe of the 3D magnetic structure beyond the capabilities of conventional imaging [121]. Another notable application of polarimetry in astronomy is that solar activities can be monitored by exploiting the circular polarization state of light [122]. Therefore, polarimetry enables highly efficient image acquisition of spatial structures of astronomical bodies compared to conventional adaptive imaging with telescopes. Fig. 9(b) shows the polarization-sensitive images of the exoplanet DH Tau b [123]. The images from left to right represent the images with unpolarized light, polarized light, and images with polarization angle. Compared to conventional imaging, additional exoplanet DH Tau b features can be captured with polarization-sensitive imaging.

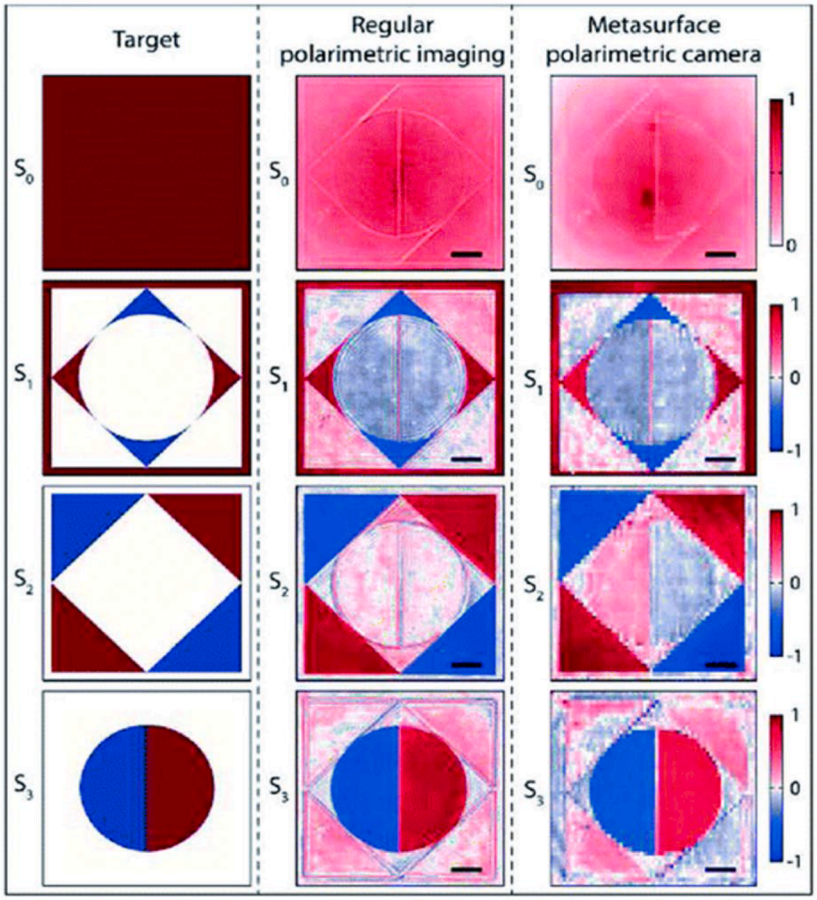

(a)

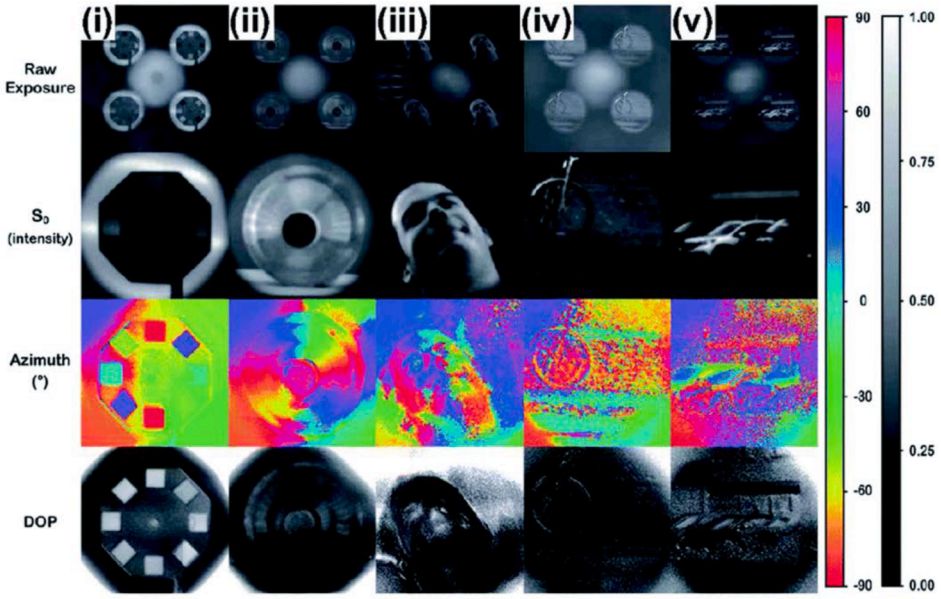

(b)

Fig. 8. Polarimetric imaging results using a metasurface-enabled polarization camera. **(a)** The target image (polarization mask) was captured using conventional polarimetry and metasurface polarimetric camera. **(b)** Full-stokes polarization images based on a metasurface polarization camera without any conventional polarization optics and moving components. (i–iii) Indoor and (iv and v) outdoor photographs with raw exposure, S_0, azimuth of polarization ellipse, and degree of polarization (DOP). (*adapted from* [111] *under Creative Commons Attribution license 4.0*).

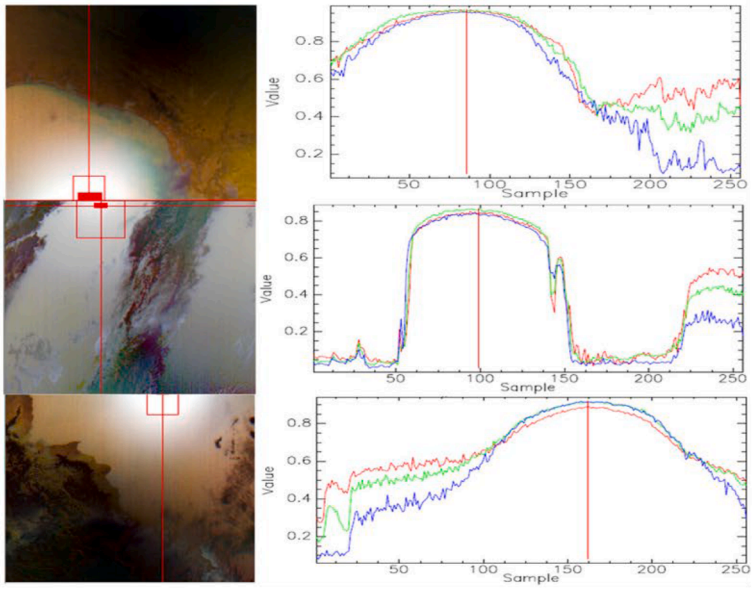

(a)

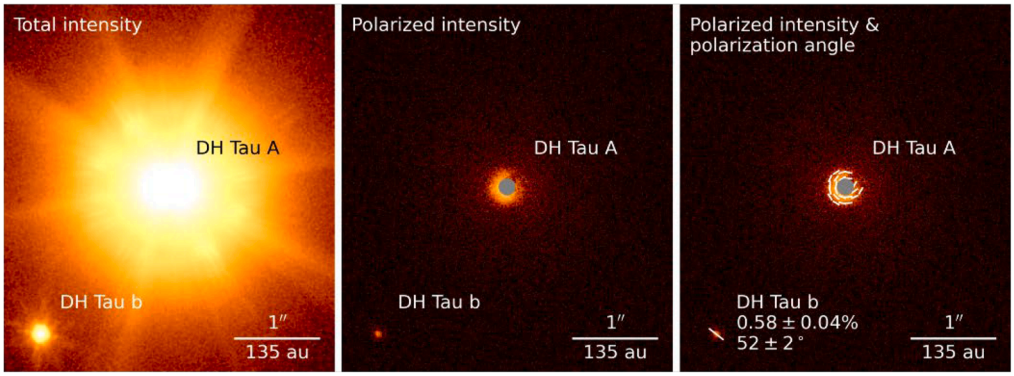

(b)

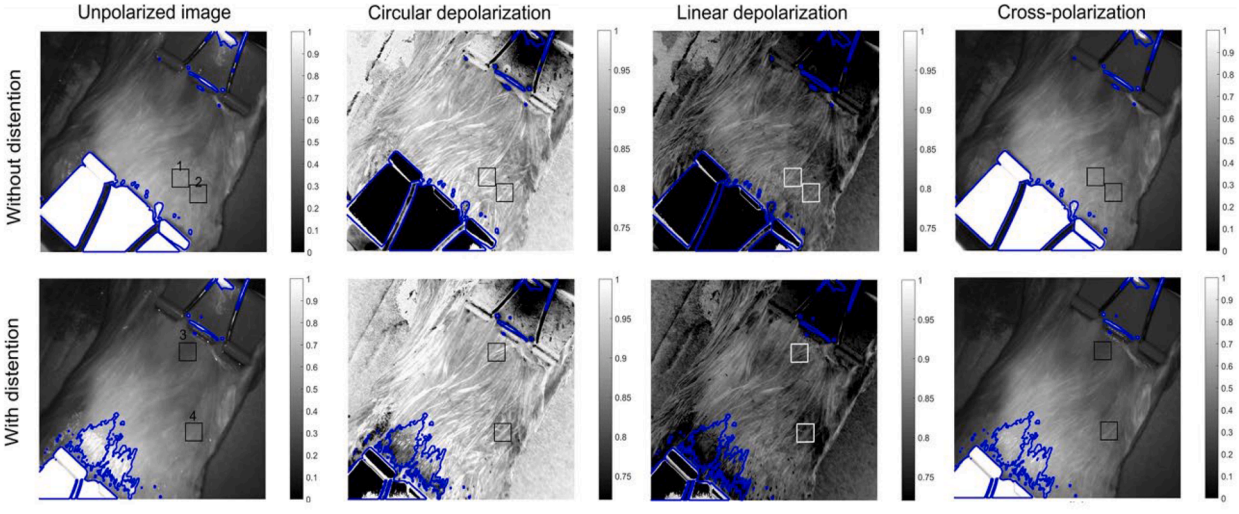

(c)

Fig. 9. Applications of polarization imaging. **(a)** Remote sensing: measured Degree of Linear Polarization (DoLP) of the sunlight region. The left image is the color image composited of 565 nm, 670 nm, and 865 nm, and the right image corresponds to DoLP plots. (*adapted from* [119] *under Creative Commons Attribution license 4.0*). **(b)** Astronomy: polarization-sensitive images of the exoplanet DH Tau b [123], **(c)** Biomedical imaging: Polarization-sensitive imaging for bladder distention diagnosis using Mueller polarimetric endoscope. (*adapted from* [128] *under Creative Commons Attribution license 4.0*).

6.3. Biomedical and clinical diagnosis

Polarimetry has exciting applications in the biomedical imaging domain, such as diagnosing and treating diseases [8,72]. Many polarization techniques have been developed for decades in biological and clinical research, each based on measurement and manipulation of the polarization of light or the vectorial transformations imposed on light by a target sample [71,124]. Polarimetric techniques, such as MMI and JMI, are prominent diagnostic tools in biomedical imaging. The morphological properties of the target sample can be correlated with the polarization properties, such as depolarization, retardance, polarizance, etc., using the Mueller matrix. On the other hand, the Jones matrix enables the extraction of in-depth phase information of the target sample, which can be utilized in tomography [125,126]. Another noteworthy application of biomedical polarimetry is polarization-resolved microscopy, which provides highly resolved images of biological target samples by optimizing the contrast and other imaging characteristics [42,47,127]. An interesting application of polarization in biomedical imaging is shown in Fig. 9(c). The influence of bladder distention is examined by measuring and comparing the distinct polarization parameters for normal and distended bladder using a polarization-sensitive endoscope [128].

7. Emerging trends, challenges, and future perspectives

Despite numerous advantages, traditional polarimetry has substantial bottlenecks. It requires bulky optical components such as polarizers, beam-splitters, wave plates, etc., which hinders its applicability in real-time imaging systems. However, attempts have been made in recent years to circumvent such limitations. For instance, advanced manufacturing techniques led to the development of optical metasurfaces. Metasurface-enabled polarimetry is the emerging domain in polarization optics. In recent years, researchers have developed various polarization-sensitive metasurfaces, which circumvent the existing issues in traditional polarimetry and enable new possibilities for advanced imaging systems and holography. For instance, diffraction grating for polarization control [129,130], polarization holograms for encoding vectorial information of light [48,131,132], chiral lenses for innovative applications [133,134], Jones-plates [60], etc. The integration of optical metasurfaces in traditional polarimetry has led to the miniaturization of conventional imaging systems and optimized polarization control. In addition, biomedical applications of polarimetry have also gained substantial attention from the research fraternity in recent years. Polarimetric techniques, such as Mueller-Stokes polarimetry, Jones phase microscopy, and optical coherence tomography (OCT), have been harnessed for the non-invasive diagnosis of severe malignancies and tissue polarimetry [55,78,79]. Some of the recent breakthroughs in this direction are hyperspectral polarimetry [135,136], OCT with automation [137,138], polarization endoscopy [128], and Mueller-matrix colposcopy [139]. Over the years, the potential applications of polarimetry have expanded drastically to multiple fields. The key emerging applications of polarization imaging can be manifested in quantum computing [108,140], nanoscale optical sensing [141], and AR/VR display technology [142,143]. However, efficient polarization control and manipulation are essential criteria for these advanced technologies and are the need of the hour. The integration of polarimetry with rapidly growing advanced technologies, such as machine learning (ML), metasurface-holography, and advanced nanoscale optical sensing, can be the future prospects of polarimetry, and attempts should be put forward in this direction.

8. Summary

This paper reviews the advances in polarization imaging from the fundamental to the advanced level. The review article offers a self-contained tutorial (reference text) in polarization optics, covering the essential elements, such as historical development, theoretical concepts, and experimental aspects of polarization imaging, followed by a brief introduction to traditional and modern polarization imaging instruments. Polarization techniques, i.e., Jones matrix imaging and Mueller-Stokes polarimetry, are thoroughly discussed in the framework of recent developments in these polarimetric techniques. Further, this review circumvents the commonly used polarization instruments, i.e., Stokes polarimeter, LC-SLM, polarization camera, etc. In addition to the historical, conceptual, and applied overview of polarimetry, the emerging research trends, associated challenges, and future prospects of polarization imaging as a multimodal combination with advanced technologies have been discussed in the subsequent section. This article targets interested readers from beginners to advanced levels, and it is expected to be useful as an easy-to-understand reference for interested readers from multidisciplinary research backgrounds.

Funding

Horizon 2020 Framework Programme (857627, CIPHR).

CRediT authorship contribution statement

Vipin Tiwari: Writing – review & editing, Writing – original draft, Visualization, Validation, Investigation, Formal analysis, Conceptualization.

Declaration of competing interest

The authors declare that they have no known competing financial interests or personal relationships that could have appeared to influence the work reported in this paper.

Data availability

No data was used for the research described in the article.

References

[1] Tyo JS, Goldstein DH, Chenault DB, Shaw JA. Polarization in Remote sensing-introduction. Appl Opt 2006. https://doi.org/10.1364/AO.45.005451.
[2] Snik F, Craven-Jones J, Escuti M, Fineschi S, Harrington D, De Martino A, et al. An overview of polarimetric sensing techniques and technology with applications to different research fields. Polariz. Meas. Anal. Remote Sens. XI 2014. https://doi.org/10.1117/12.2053245.
[3] Piironen J. Astronomical polarimetry. Icarus; 1997. https://doi.org/10.1006/icar.1997.5741.
[4] Polarimetry Hough J. A powerful diagnostic tool in astronomy. Astron Geophys 2006. https://doi.org/10.1111/j.1468-4004.2006.47331.x.
[5] Fade J, Roche M, Alouini M. Computational polarization imaging from a single speckle image. Opt Lett 2012. https://doi.org/10.1364/ol.37.000386.
[6] Wang J, Xu G, Ma J, Wang Y, Li Y. Polarization computational imaging super-resolution reconstruction with lightweight attention cascading network. Guangxue Jingmi Gongcheng/Optics Precis Eng 2022. https://doi.org/10.37188/OPE.20223019.2404.
[7] Tiwari V, Bisht NS. Extended depth of field of a diffraction limited imaging system using a spatial light modulator based intensity compensated polarization coded aperture. Opt Contin 2023;2:1. https://doi.org/10.1364/optcon.459450.
[8] Ghosh N. Tissue polarimetry: concepts, challenges, applications, and outlook. J Biomed Opt 2011. https://doi.org/10.1117/1.3652896.
[9] Qi J, Elson DS. Mueller polarimetric imaging for surgical and diagnostic applications: a review. J Biophotonics 2017;10:950–82. https://doi.org/10.1002/jbio.201600152.
[10] He C, He H, Chang J, Chen B, Ma H, Booth MJ. Polarisation optics for biomedical and clinical applications: a review. Light Sci Appl 2021;10. https://doi.org/10.1038/s41377-021-00639-x.
[11] Luo H, Cao J, Gai X, Ding Q. Industrial vision based on polarization imaging and its key technologies. Laser Optoelectron Prog 2022. https://doi.org/10.3788/LOP202259.1415002.
[12] Tiwari VS, Bisht N. Spatial light modulators and their applications in polarization holography. Hologr. - Recent Adv. Appl. 2023. https://doi.org/10.5772/intechopen.107110.
[13] Goldstein D.H. Polarized light: third edition. 2017. https://doi.org/10.1201/b10436.

[14] Munro PRT. Introduction to the theory of Coherence and Polarization of light. by E. Wolf.. Contemp phys. 2009. https://doi.org/10.1080/00107510902910348.
[15] Chekhova M., Banzer P. Polarization of light: in classical, quantum, and nonlinear optics. 2021. https://doi.org/10.1515/9783110668025.
[16] Li X, Liu Z, Cai Y, Pan C, Song J, Wang J, et al. Polarization 3D imaging technology: a review. Front Phys 2023. https://doi.org/10.3389/fphy.2023.1198457.
[17] Erasmus Bartholin. Experiments with the double refracting Iceland crystal which led to the discovery of a marvelous and strange refraction. [Westtown, Pa.], Brandt; 1959.
[18] Graubard M. Christian Huygens and the development of science in the seventeenth century. A. E. Bell . Isis 1949;40:272–3. https://doi.org/10.1086/349052.
[19] Kahr B, Claborn K. The lives of Malus and his bicentennial law. ChemPhysChem 2008;9:43–58. https://doi.org/10.1002/cphc.200700173.
[20] Brewster D. On the laws which regulate the polarisation of light by reflexion from transparent bodies. Philos Trans R Soc London 1815;105:125–59.
[21] Fresnel A.J. Oeuvres Complétes d'Augustin Fresn n.d.;767.
[22] Strutt JWXV. On the light from the sky, its polarization and colour. London, Edinburgh. Dublin Philos Mag J Sci 1871. https://doi.org/10.1080/14786447108640452.
[23] Piller H. Faraday rotation. Semicond semimetals 1972. https://doi.org/10.1016/S0080-8784(08)62344-3.
[24] Schmidt K -HT. Planets, stars and nebulae studied with photopolarimetry. GEHRELS. Tuscon, Arizona: University of Arizona Press; 1974. https://doi.org/10.1002/asna.19762970317. XVI + 133 Seiten. Preis $ 17.50. Astron Nachrichten 1976.
[25] Thompson SP. The inventor of the Nicol prism [1]. Nature 1906. https://doi.org/10.1038/073340d0.
[26] Land EH. Some aspects of the development of sheet polarizers*. J Opt Soc Am 1951. https://doi.org/10.1364/josa.41.000957.
[27] Brosseau C. Polarization and coherence optics: historical perspective, status, and future directions. Prog. Opt. 2010. https://doi.org/10.1016/S0079-6638(10)05408-9.
[28] Stokes G. On the composition and resolution of streams of polarized light from different sources. Cambridge: Cambridge Philosophical Society; 1852.
[29] Stokes GG. On the composition and resolution of streams of polarized light from different sources. Math. Phys. Pap. 2010:233–58. https://doi.org/10.1017/cbo9780511702266.010.
[30] Jekrard HG. Transmission of light through birefringent and optically active Media: the Poincaré Sphere. J Opt Soc Am 1954;44:634. https://doi.org/10.1364/josa.44.000634.
[31] Mueller H. The foundation of optics. J Opt Soc Am 1948.
[32] Jones RC. A new calculus for the treatment of optical SystemsIII the Sohncke theory of optical activity. J Opt Soc Am 1941;31:500. https://doi.org/10.1364/josa.31.000500.
[33] JONES RC. A new calculus for the treatment of optical systems. IV. J Opt Soc Am 1942;32:486–93.
[34] Jones RC. A new calculus for the treatment of optical SystemsV A more general formulation, and description of another calculus. J Opt Soc Am 1947;37:107. https://doi.org/10.1364/josa.37.000107.
[35] Jones RC. A new calculus for the treatment of optical systems VII properties of the N-matrices. J Opt Soc Am 1948;38:671. https://doi.org/10.1364/josa.38.000671.
[36] Lohmann AW. Reconstruction of vectorial wavefronts. Appl Opt 1965. https://doi.org/10.1364/ao.4.001667.
[37] Colomb T, Dahlgren P, Beghuin D, Cuche E, Marquet P, Depeursinge C. Polarization imaging by use of digital holography. Appl Opt 2002. https://doi.org/10.1364/ao.41.000027.
[38] Kuroda K, Matsuhashi Y, Fujimura R, Shimura T. Theory of polarization holography. Opt Rev 2011. https://doi.org/10.1007/s10043-011-0072-5.
[39] Singh RK, Naik DN, Itou H, Miyamoto Y, holography Takeda MStokes. Opt Lett 2012. https://doi.org/10.1364/ol.37.000966.
[40] Brasselet S, Alonso MA. Polarization microscopy: from ensemble structural imaging to single-molecule 3D orientation and localization microscopy. Optica 2023. https://doi.org/10.1364/optica.502119.
[41] Le Gratiet A, Mohebi A, Callegari F, Bianchini P, Diaspro A. Review on complete mueller matrix optical scanning microscopy imaging. Appl Sci 2021. https://doi.org/10.3390/app11041632.
[42] dos Anjos EHM, Mello MLS, Vidal B, de C. High-performance polarization microscopy reveals structural remodeling in rat calcaneal tendons cultivated In vitro. Cells 2023. https://doi.org/10.3390/cells12040566.
[43] Hao X, Kuang C, Wang T, Liu X. Effects of polarization on the de-excitation dark focal spot in STED microscopy. J Opt 2010. https://doi.org/10.1088/2040-8978/12/11/115707.
[44] Rimoli CV, Valades-Cruz CA, Curcio V, Mavrakis M, Brasselet S. 4polar-STORM polarized super-resolution imaging of actin filament organization in cells. Nat Commun 2022. https://doi.org/10.1038/s41467-022-27966-w.
[45] Balthasar Mueller JP, Rubin NA, Devlin RC, Groever B, Capasso F. Metasurface polarization optics: independent phase control of arbitrary orthogonal states of polarization. Phys Rev Lett 2017. https://doi.org/10.1103/PhysRevLett.118.113901.
[46] Rubin NA, Shi Z, Capasso F. Polarization in diffractive optics and metasurfaces. Adv Opt Photonics 2021. https://doi.org/10.1364/aop.439986.
[47] Spandana KU, Mahato KK, Mazumder N. Polarization-resolved Stokes-Mueller imaging: a review of technology and applications. Lasers Med Sci 2019;34:1283–93. https://doi.org/10.1007/s10103-019-02752-1.
[48] Hong YF, Zang JL, Liu Y, Fan FL, Wu AA, Shao L, et al. Review and prospect of polarization holography. Chinese Opt 2017;10:588–602. https://doi.org/10.3788/CO.20171005.0588.
[49] Gautam SK, Panchal P, Mishra P, Naik DN, Narayanamurthy CS, Singh RK. Single-shot Jones Matrix microscopy. Springer Proc. Phys. 2021;258:557–60. https://doi.org/10.1007/978-981-15-9259-1_128.
[50] Hunte C. The {Jones-Mueller} transformation. Fiz A 2008;17:51–8.
[51] Wang Z, Millet LJ, Gillette MU, Popescu G. Jones phase microscopy of transparent and anisotropic samples. Opt Lett 2008;33:1270. https://doi.org/10.1364/ol.33.001270.
[52] Kim Y, Jeong J, Jang J, Kim MW, Park Y. Polarization holographic microscopy for extracting spatio-temporally resolved Jones matrix. Opt Express 2012. https://doi.org/10.1364/oe.20.009948.
[53] Park J, Yu H, Park J-H, Park Y. LCD panel characterization by measuring full Jones matrix of individual pixels using polarization-sensitive digital holographic microscopy. Opt Express 2014. https://doi.org/10.1364/oe.22.024304.
[54] Sreelal MM, Vinu RV, Singh RK. Jones matrix microscopy from a single-shot intensity measurement. Opt Lett 2017. https://doi.org/10.1364/ol.42.005194.
[55] Liu H, Vinu RV, Chen K, Liao D, Chen Z, Pu J. Real-time Jones matrix synthesis by compact polarization inline holographic microscopy. Laser Photonics Rev 2024. https://doi.org/10.1002/lpor.202301261.
[56] Liu X, Wang B-Y, Guo C-S. One-step Jones matrix polarization holography for extraction of spatially resolved Jones matrix of polarization-sensitive materials. Opt Lett 2014;39:6170. https://doi.org/10.1364/ol.39.006170.
[57] Yang TD, Park K, Kang YG, Lee KJ, Kim B-M, Choi Y. Single-shot digital holographic microscopy for quantifying a spatially-resolved Jones matrix of biological specimens. Opt Express 2016. https://doi.org/10.1364/oe.24.029302.
[58] Cheng Z, Zhang Y, Liu X, Guo C, He C, Liu G, et al. Time-resolved four-channel Jones matrix measurement of birefringent materials using an ultrafast laser. Materials (Basel) 2022. https://doi.org/10.3390/ma15217813.
[59] Liu X, Wang B-Y, Guo C-S. One-step Jones matrix polarization holography for extraction of spatially resolved Jones matrix of polarization-sensitive materials. Opt Lett 2014. https://doi.org/10.1364/ol.39.006170.
[60] Rubin NA, Zaidi A, Dorrah AH, Shi Z, Capasso F. Jones matrix holography with metasurfaces. Sci Adv 2021. https://doi.org/10.1126/sciadv.abg7488.
[61] Ambirajan A. Optimum angles for a polarimeter: part I. Opt Eng 1995. https://doi.org/10.1117/12.202093.
[62] Peinado A, Lizana A, Vidal J, Iemmi C, Campos J. Optimized stokes polarimeters based on a single twisted nematic liquid-crystal device for the minimization of noise propagation. Appl Opt 2011. https://doi.org/10.1364/AO.50.005437.
[63] Capobianco G, Fineschi S, Massone G, Balboni E, Malvezzi AM, Crescenzio G, et al. Electro-optical polarimeters for ground-based and space-based observations of the solar K-corona. Mod. Technol. Space- Ground-based Telesc. Instrum. II 2012. https://doi.org/10.1117/12.926896.
[64] FitzGerald WR, Hore DK. Photoelastic modulator-based broadband mid-infrared Stokes polarimeter. J Mod Opt 2018. https://doi.org/10.1080/09500340.2017.1377303.
[65] Azzam RMA. Division-of-amplitude photopolarimeter (DOAP) for the simultaneous measurement of all four stokes parameters of light. Opt Acta (Lond) 1982. https://doi.org/10.1080/713820903.
[66] Azzam RMA. Instrument matrix of the four-detector photopolarimeter: physical meaning of its rows and columns and constraints on its elements. J Opt Soc Am A 1990. https://doi.org/10.1364/josaa.7.000087.
[67] Azzam RMA. An arrangement of two reflective photodetectors for measuring all four Stokes parameters of light. Rev Sci Instrum 1991. https://doi.org/10.1063/1.1142370.
[68] Azzam RMA. Arrangement of four photodetectors for measuring the state of polarization of light. Opt Lett 1985. https://doi.org/10.1364/ol.10.000309.
[69] Tokuda T, Sato S, Yamada H, Sasagawa K, Ohta J. Polarisation-analysing CMOS photosensor with monolithically embedded wire grid polariser. Electron Lett 2009. https://doi.org/10.1049/el:20093132.
[70] Gruev V, Perkins R, York T. CCD polarization imaging sensor with aluminum nanowire optical filters. Opt Express 2010. https://doi.org/10.1364/oe.18.019087.
[71] Sheng W, Li W, Qi J, Liu T, He H, Dong Y, et al. Quantitative analysis of 4 × 4 mueller matrix transformation parameters for biomedical imaging. Photonics 2019. https://doi.org/10.3390/PHOTONICS6010034.
[72] Qi J, Elson DS. Mueller polarimetric imaging for surgical and diagnostic applications: a review. J Biophotonics 2017. https://doi.org/10.1002/jbio.201600152.
[73] Tiwari V, Pandey Y, Bisht NS. Spatially addressable polarimetric calibration of reflective-type spatial light modulator using mueller–Stokes polarimetry. Front Phys 2021. https://doi.org/10.3389/fphy.2021.709192.
[74] Gottlieb D, Arteaga O. Mueller matrix imaging with a polarization camera: application to microscopy. Opt Express 2021. https://doi.org/10.1364/oe.439529.
[75] Le Gratiet A, Mohebi A, Callegari F, Bianchini P, Diaspro A. Review on complete mueller matrix optical scanning microscopy imaging. Appl Sci 2021;11:1–18. https://doi.org/10.3390/app11041632.
[76] Zaidi A, Rubin NA, Meretska ML, Li LW, Dorrah AH, Park J-S, et al. Metasurface-enabled single-shot and complete Mueller matrix imaging. Nat Photonics 2024;18:704–12. https://doi.org/10.1038/s41566-024-01426-x.

[77] Tiwari V, Gautam SK, Naik DN, Singh RK, Bisht NS. Characterization of a spatial light modulator using polarization-sensitive digital holography. Appl Opt 2020. https://doi.org/10.1364/ao.380572.

[78] de Boer JF, Hitzenberger CK, Yasuno Y. Polarization sensitive optical coherence tomography – a review [Invited]. Biomed Opt Express 2017. https://doi.org/10.1364/boe.8.001838.

[79] Yasuno Y. Multi-contrast Jones-matrix optical coherence tomography - the concept, principle, implementation, and applications. IEEE J Sel Top Quantum Electron 2023. https://doi.org/10.1109/JSTQE.2023.3248148.

[80] Rubin NA, D'Aversa G, Chevalier P, Shi Z, Chen WT, Capasso F. Matrix fourier optics enables a compact full-stokes polarization camera. Science (80-) 2019. https://doi.org/10.1126/science.aax1839.

[81] Gong S, Meng Y, Wang C, Chen Y, Meng X, Wu W, et al. Full-stokes polarimetry based on rotating metasurfaces. Appl Phys Lett 2022. https://doi.org/10.1063/5.0078097.

[82] Tiwari V, Bisht NS. Combined Jones–Stokes polarimetry and its decomposition into associated anisotropic characteristics of spatial light modulator. Photonics 2022;9. https://doi.org/10.3390/photonics9030195.

[83] Rodenhuis M, Snik F, van Harten G, Hoeijmakers J, Keller CU. Five-dimensional optical instrumentation: combining polarimetry with time-resolved integral-field spectroscopy. Polariz. Meas. Anal. Remote Sens. XI 2014. https://doi.org/10.1117/12.2053241.

[84] Mu T, Han F, Li H, Tuniyazi A, Li Q, Gong H, et al. Snapshot hyperspectral imaging polarimetry with full spectropolarimetric resolution. Opt Lasers Eng 2022. https://doi.org/10.1016/j.optlaseng.2021.106767.

[85] Zhang Y., Wang C., Liu X., Xu Z., Zhang Q., Yue Q., et al. Snapshot compressive hyperspectral imaging via polarization conversion metasurface, 2023. https://doi.org/10.1117/12.2687117.

[86] da Chiu L, AF Palonpon, Smith NI, Kawata S, Sodeoka M, Fujita K. Dual-polarization Raman spectral imaging to extract overlapping molecular fingerprints of living cells. J Biophotonics 2015. https://doi.org/10.1002/jbio.201300204.

[87] Hsiang EL, Wu ST. Novel developments in computational spectropolarimeter. Light Sci Appl 2023. https://doi.org/10.1038/s41377-023-01097-3.

[88] Meng X, Li J, Xu T, Liu D, Zhu R. High throughput full Stokes Fourier transform imaging spectropolarimetry. Opt Express 2013. https://doi.org/10.1364/oe.21.032071.

[89] Vasefi F, MacKinnon N, Saager RB, Durkin AJ, Chave R, Lindsley EH, et al. Polarization-sensitive hyperspectral imaging in vivo: a multimode dermoscope for skin analysis. Sci Rep 2014. https://doi.org/10.1038/srep04924.

[90] Zhou X, Ma L, Mubarak HK, Palsgrove D, Sumer BD, Chen AY, et al. Polarized hyperspectral microscopic imaging system for enhancing the visualization of collagen fibers and head and neck squamous cell carcinoma. J Biomed Opt 2024. https://doi.org/10.1117/1.jbo.29.1.016005.

[91] Jones SH, Iannarilli FJ, Kebabian PL, Conant JA. The Hyperspectral Polarimeter for Aerosol retrievals (HySPAR): a new instrument for passive remote sensing of aerosols. In: 2005 IEEE Work. Remote Sens. Atmos. Aerosols; 2005. https://doi.org/10.1109/AERSOL.2005.1494149.

[92] Sushkevich TA, Falaleeva VA. Hyperspectral model of solar radiation transport in an atmosphere with cirrus clouds. Izv - Atmos Ocean Phys 2021. https://doi.org/10.1134/S0001433821030105.

[93] Iglesias FA, Feller A. Instrumentation for solar spectropolarimetry: state of the art and prospects. Opt Eng 2019. https://doi.org/10.1117/1.oe.58.8.082417.

[94] Ceolato R, Riviere N. Spectral polarimetric light-scattering by particulate media: 1. Theory of spectral vector radiative transfer. J Quant Spectrosc Radiat Transf 2016. https://doi.org/10.1016/j.jqsrt.2015.12.026.

[95] Yao H, Fu B, Zhang Y, Li S, Xie S, Qin J, et al. Combination of hyperspectral and quad-polarization SAR images to classify marsh vegetation using stacking ensemble learning algorithm. Remote Sens 2022. https://doi.org/10.3390/rs14215478.

[96] Fan A, Xu T, Teng G, Wang X, Zhang Y, Pan C. Hyperspectral polarization-compressed imaging and reconstruction with sparse basis optimized by particle swarm optimization. Chemom Intell Lab Syst 2020. https://doi.org/10.1016/j.chemolab.2020.104163.

[97] Fan A, Xu T, Teng G, Wang X, Xu C, Zhang Y, et al. Deep learning reconstruction enables full-stokes single compression in polarized hyperspectral imaging. Chinese Opt Lett 2023. https://doi.org/10.3788/col202321.051101.

[98] Zhang L, Zhou C, Liu B, Ding Y, Ahn HJ, Chang S, et al. Real-time machine learning–enhanced hyperspectro-polarimetric imaging via an encoding metasurface. Sci Adv 2024;10:5192. https://doi.org/10.1126/SCIADV.ADP5192/SUPPL_FILE/SCIADV.ADP5192_MOVIES_S1_AND_S2.ZIP.

[99] Vedel M, Breugnot S, Lechocinski N. Full Stokes polarization imaging camera. Polariz. Sci. Remote Sens. V 2011. https://doi.org/10.1117/12.892491.

[100] Cox MA, Rosales-Guzmán C. Real-time stokes polarimetry using a polarization camera. Appl Opt 2023. https://doi.org/10.1364/ao.504249.

[101] Arbabi E, Kamali SM, Arbabi A, Faraon A. Full-stokes imaging polarimetry using dielectric metasurfaces. ACS Photonics 2018. https://doi.org/10.1021/acsphotonics.8b00362.

[102] Zhang S, Huang L, Li X, Zhao R, Wei Q, Zhou H, et al. Dynamic display of full-stokes vectorial holography based on metasurfaces. ACS Photonics 2021. https://doi.org/10.1021/acsphotonics.1c00307.

[103] Yang Y, Forbes A, Cao L. A review of liquid crystal spatial light modulators: devices and applications. Opto-Electronic Sci 2023. https://doi.org/10.29026/oes.2023.230026.

[104] Manisha Tiwari V, Bisht NS, Singh RK. A compact and lens less digital holography setup for polarimetric analysis of spatial light modulator. Opt Laser Technol 2023;167:109748. https://doi.org/10.1016/j.optlastec.2023.109748.

[105] Kumar P, Nishchal NK. Phase response optimization of a liquid crystal spatial light modulator with partially coherent light. Appl Opt 2021;60:10795. https://doi.org/10.1364/ao.439654.

[106] Chandra AD, Banerjee A. Rapid phase calibration of a spatial light modulator using novel phase masks and optimization of its efficiency using an iterative algorithm. J Mod Opt 2020. https://doi.org/10.1080/09500340.2020.1760954.

[107] Zhao R, Huang L, Wang Y. Recent advances in multi-dimensional metasurfaces holographic technologies. PhotoniX 2020. https://doi.org/10.1186/s43074-020-00020-y.

[108] Shi Z, Zhu AY, Li Z, Huang YW, Huang YW, Chen WT, et al. Continuous angle-tunable birefringence with freeform metasurfaces for arbitrary polarization conversion. Sci Adv 2020;6. https://doi.org/10.1126/sciadv.aba3367.

[109] Zhou H, Sain B, Wang Y, Schlickriede C, Zhao R, Zhang X, et al. Polarization-encrypted orbital angular momentum multiplexed metasurface holography. ACS Nano 2020;14:5553–9. https://doi.org/10.1021/acsnano.9b09814.

[110] Rubin NA, Shi Z, Capasso F. Polarization in diffractive optics and metasurfaces. Adv Opt Photonics 2021;13:836. https://doi.org/10.1364/aop.439986.

[111] Lee D, Gwak J, Badloe T, Palomba S, Rho J. Metasurfaces-based imaging and applications: from miniaturized optical components to functional imaging platforms. Nanoscale Adv 2020. https://doi.org/10.1039/c9na00751b.

[112] Praja MP, Pamungkas W. Linear polarization on radar cross section measurement for tank miniature. J INFOTEL 2022. https://doi.org/10.20895/infotel.v14i4.782.

[113] Fei L, Shaojie S, Pingli H, Kui Y, Xiaopeng S. Development of underwater polarization imaging technology. Laser optoelectron prog. 2021. https://doi.org/10.3788/LOP202158.0600001.

[114] Pust NJ, Shaw JA. Dual-field imaging polarimeter using liquid crystal variable retarders. Appl Opt 2006. https://doi.org/10.1364/AO.45.005470.

[115] Dubovik O, Li Z, Mishchenko MI, Tanré D, Karol Y, Bojkov B, et al. Polarimetric remote sensing of atmospheric aerosols: instruments, methodologies, results, and perspectives. J Quant Spectrosc Radiat Transf 2019. https://doi.org/10.1016/j.jqsrt.2018.11.024.

[116] Mao S, Wang A, Yi Y, Yin Z, Zhao Y, Hu X, et al. Polarization Raman lidar for atmospheric correction during remote sensing satellite calibration: instrument and test measurements. Opt Express 2022. https://doi.org/10.1364/oe.453499.

[117] Deschamps PY, Buriez JC, Bréon FM, Leroy M, Podaire A, Bricaud A, et al. The POLDER mission: instrument characteristics and scientific objectives. IEEE Trans Geosci Remote Sens 1994. https://doi.org/10.1109/36.297978.

[118] Diner DJ, Davis A, Hancock B, Geier S, Rheingans B, Jovanovic V, et al. First results from a dual photoelastic-modulator-based polarimetric camera. Appl Opt 2010. https://doi.org/10.1364/AO.49.002929.

[119] Wang H, Zhang P, Yin D, Li Z, Shang H, Xu H, et al. Shortwave Infrared Multi-angle polarization imager (MAPI) onboard Fengyun-3 precipitation satellite for enhanced cloud characterization. Remote Sens 2022. https://doi.org/10.3390/rs14194855.

[120] Redfern M. Astronomical polarimetry in the new era – applications and challenges. EPJ web conf. 2010. https://doi.org/10.1051/epjconf/20100505005.

[121] Snik F, Keller CU. Astronomical polarimetry: polarized views of stars and planets. Planets, stars stellar syst. Astron. Tech. Software, Data 2013;Vol. 2. https://doi.org/10.1007/978-94-007-5618-2_4.

[122] Rodenhuis M, Canovas H, Jeffers SV, de Juan Ovelar M, Min M, Homs L, et al. The extreme polarimeter: design, performance, first results and upgrades. Ground-based Airborne Instrum. Astron. IV 2012. https://doi.org/10.1117/12.927203.

[123] van Holstein RG, Stolker T, Jensen-Clem R, Ginski C, Milli J, de Boer J, et al. A survey of the linear polarization of directly imaged exoplanets and brown dwarf companions with SPHERE-IRDIS. Astron Astrophys 2021. https://doi.org/10.1051/0004-6361/202039290.

[124] Rehbinder J, Haddad H, Deby S, Teig B, Nazac A, Novikova T, et al. Ex vivo Mueller polarimetric imaging of the uterine cervix: a first statistical evaluation. J Biomed Opt 2016;21:071113. https://doi.org/10.1117/1.jbo.21.7.071113.

[125] Palawong K, Sonsupap S, Maensiri S, Meemon P. Polarization sensitive optical coherence tomography for materials characterization. Chiang Mai J Sci 2018.

[126] Wang J, Chaney EJ, Aksamitiene E, Marjanovic M, Boppart SA. Computational adaptive optics for polarization-sensitive optical coherence tomography. Opt Lett 2021;46:2071. https://doi.org/10.1364/ol.418637.

[127] Dutra RS, Viana NB, Maia Neto PA, Nussenzveig HM. Polarization effects in optical tweezers. J Opt A Pure Appl Opt 2007. https://doi.org/10.1088/1464-4258/9/8/S15.

[128] Qi J, Elson DS. A high definition Mueller polarimetric endoscope for tissue characterisation. Sci Rep 2016. https://doi.org/10.1038/srep25953.

[129] Stafeev SS, Nalimov AG, O'Faolain L, Kotlyar MV. Binary diffraction gratings for controlling polarization and phase of laser light [review]. Comput Opt 2017. https://doi.org/10.18287/2412-6179-2017-41-3-299-314.

[130] Wei R, Zang J, Liu Y, Fan F, Huang Z, Zhu L, et al. Review on polarization holography for high density storage. Guangdian Gongcheng/Opto-Electronic Eng 2019;46. https://doi.org/10.12086/oee.2019.180598.

[131] Deng ZL, Wang ZQ, Li FJ, Hu MX, Li X. Multi-freedom metasurface empowered vectorial holography. Nanophotonics 2022;11:1725–39. https://doi.org/10.1515/nanoph-2021-0662.

[132] Hermon S, Ma A, Yue F, Kubrom F, Intaravanne Y, Han J, et al. Metasurface hologram for polarization measurement. Opt Lett 2019. https://doi.org/10.1364/ol.44.004436.

[133] Groever B, Rubin NA, Mueller JPB, Devlin RC, Capasso F. High-efficiency chiral meta-lens. Sci Rep 2018. https://doi.org/10.1038/s41598-018-25675-3.
[134] Perera K, Haputhantrige N, Himel MSH, Mostafa M, Adaka A, Mann EK, et al. Electrically tunable polymer stabilized chiral ferroelectric nematic liquid crystal microlenses. Adv Opt Mater 2024. https://doi.org/10.1002/adom.202302500.
[135] Li Q, Wang Q, Lu F, Cao Y, Zhao X. Lenslet-array-based snapshot hyperspectral imaging polarimeter using opposite spectral modulation. Opt Lasers Eng 2024. https://doi.org/10.1016/j.optlaseng.2023.107939.
[136] Sun L, Lucey PG, Honniball CI, Sandford M, Costello ES, Burkhard L, et al. Hyperspectral polarimetry of eight Apollo soils. Icarus 2022. https://doi.org/10.1016/j.icarus.2021.114740.
[137] Al-Falahi Z, Tran H, Middleton P, Basilakis J, Lo S, Dang V, et al. Automation of optical coherence tomography (OCT) tissued morphology and vessel sizing with artificial intelligence. Hear Lung Circ 2022. https://doi.org/10.1016/j.hlc.2022.06.561.
[138] Venkatraman K, Sumathi M. Automations in oct imaging – A tool in analysis of fluid based retinal abnormalities. Int J Sci Technol Res 2020.
[139] Chue-Sang J, Holness N. Use of Mueller matrix colposcopy in the characterization of cervical collagen anisotropy. J Biomed Opt 2018. https://doi.org/10.1117/1.jbo.23.12.121605.
[140] Samanta D. Implementation of polarization-encoded quantum Fredkin gate using Kerr effect. J Opt Commun 2023. https://doi.org/10.1515/joc-2019-0077.
[141] Nguyen TT, Han GR, Jang CH, Ju H. Optical birefringence of liquid crystals for label-free optical biosensing diagnosis. Int J Nanomedicine 2015. https://doi.org/10.2147/IJN.S88286.
[142] Guo X, Zhong J, Li B, Qi S, Li Y, Li P, et al. Full-color holographic display and encryption with Full-polarization degree of freedom. Adv Mater 2022. https://doi.org/10.1002/adma.202103192.
[143] Xiong J, Hsiang EL, He Z, Zhan T, Wu ST. Augmented reality and virtual reality displays: emerging technologies and future perspectives. Light Sci Appl 2021. https://doi.org/10.1038/s41377-021-00658-8.